AWARD NUMBER:
W81XWH-14-1-0056

TITLE:
Tumor Tension Induces Persistent Inflammation and Promotes Breast Cancer Aggression

PRINCIPAL INVESTIGATOR:
Ori Maller

CONTRACTING ORGANIZATION:
University of California, San Francisco
San Francisco CA 94103-4249

REPORT DATE:
October 2016

TYPE OF REPORT: Annual

PREPARED FOR: U.S. Army Medical Research and Materiel Command
Fort Detrick, Maryland 21702-5012

REPORT DOCUMENTATION PAGE

Form Approved
OMB No. 0704-0188

1. REPORT DATE	2. REPORT TYPE	3. DATES COVERED
October 2016	Annual	09-30-2015 to 09-29-2016

4. TITLE AND SUBTITLE

Tumor Tension Induces Persistent Inflammation and Promotes Breast Cancer Aggression

5a. CONTRACT NUMBER

5b. GRANT NUMBER
W81XWH-14-1-0056

5c. PROGRAM ELEMENT NUMBER

6. AUTHOR(S)

Ori Maller and Valerie M. Weaver

E-Mail:ori.maller@ucsf.edu

5d. PROJECT NUMBER

5e. TASK NUMBER

5f. WORK UNIT NUMBER

7. PERFORMING ORGANIZATION NAME(S) AND ADDRESS(ES)

University of California, San Francisco
1855 Folsom St STE 425
San Francisco CA 94103-4249

8. PERFORMING ORGANIZATION REPORT NUMBER

9. SPONSORING / MONITORING AGENCY NAME(S) AND ADDRESS(ES)

U.S. Army Medical Research and Materiel Command
Fort Detrick, Maryland 21702-5012

10. SPONSOR/MONITOR'S ACRONYM(S)

11. SPONSOR/MONITOR'S REPORT NUMBER(S)

12. DISTRIBUTION / AVAILABILITY STATEMENT

Approved for Public Release; Distribution Unlimited

13. SUPPLEMENTARY NOTES

14. ABSTRACT

We previously established a positive correlation between a fibrotic phenotype in human breast tumors — especially the HER2 and Basal-like breast cancer subtypes — and CD45 and CD68 positive immune cell infiltration. We are currently interested in elucidating how this fibrotic phenotype may influence the immune response. To address this question, we examined if matrix stiffness alters the function of STAT3, a central regulator of tumor inflammation. We hypothesize that tissue fibrosis promotes STAT3 signaling in mammary tumor cells, and subsequently alters cytokine milieu to induce a pro-tumor immune response.
We found that ECM stiffness directly enhanced STAT3 phosphorylation in tumor cells both i*n vitro* and *in vivo*. Our data suggest the fibrotic phenotype promotes STAT3 activity, enhancement of which may drive a pro-tumor immune response. Indeed, we observed several alterations in cytokines and immune cell populations upon STAT3 ablation consistent with anti-tumor immune response. Overall, our work reveals a novel mechanistic insight into how a pro-tumor immune response stems from the interplay between fibrosis and STAT3 signaling in tumor cells. As such, our findings may stimulate an interest in exploring combinational treatment options with anti-fibrotic agents and immunotherapy.

15. SUBJECT TERMS

Nothing listed

16. SECURITY CLASSIFICATION OF:			17. LIMITATION OF ABSTRACT	18. NUMBER OF PAGES	19a. NAME OF RESPONSIBLE PERSON
a. REPORT	b. ABSTRACT	c. THIS PAGE			USAMRMC
Unclassified	Unclassified	Unclassified	Unclassified	41	19b. TELEPHONE NUMBER *(include area code)*

Table of Contents

Introduction:

Human breast tumors are highly fibrotic and their extracellular matrices (ECMs) are stiffer relative to benign lesions. A major contributor to tumor mechanics is fibrillar collagen-rich ECM. During tumor progression, fibrillar collagen content increases and its organization is characterized by bundles of aligned collagen fibers that are oriented perpendicular, particularly on the invasive fronts in both mouse models of breast cancer and human disease. We demonstrated that a stiffened ECM and elevated mechanosignaling (e.g. β1 integrin-focal adhesion kinase signaling axis) promoted mammary tumorigenesis, whereas reducing ECM stiffening impeded tumor formation. More recently, we observed significant correlations between macrophage infiltration and ECM stiffness in luminal B and basal-like breast cancer, but not luminal A. My original hypothesis was that tumor cell tension and ECM stiffening cooperate with inflammatory signaling to facilitate immune evasion and promote breast cancer aggression. In this progress report, I present our latest data that led us to generate a refined hypothesis: macrophages promote fibrosis during early tumorigenesis that induces inflammatory signaling, resulting in a feed-forward loop to induce immune suppression and subsequently breast cancer aggression.

Keywords:

AFM	Atomic force microscopy
BAPN	beta-aminoproprionitrile
CSF	Colony stimulating factor
DOX	Doxycycline
ECM	Extracellular matrix
FAK	Focal adhesion kinase
ITGB1	Integrin β1
HLCC	Lysine aldehyde (Hyl^{ald})-derived collagen cross-links
LCC	Lysine aldehyde (Lys^{ald})-derived collagen cross-links
LIF	Leukemia inhibitory factor
IL	Interleukin
MS	Mass spectrometry
PyMT	Polyoma virus-middle T antigen
LH2	Lysyl hydroxylase 2
LOX	Lysyl Oxidase
LuBC	Luminal breast cancer
qPCR	Quantitative polymerase chain reaction
STAT3	Signal transducer and activator of transcription 3
TAM	Tumor-associated macrophages
TGFβ	Transforming growth factor β
TNBC	Triple-negative breast cancer
TuDC	Tumor-associated dendritic cells
xAAA	Cross-linked amino acid analysis

Accomplishments/Changes/Problems:

Our recent efforts focused on two fronts: first, we developed and validated in collaboration with Dr. Hansen's lab a highly specific and quantitative collagen cross-linking assay, which led us to identify a novel biomarker for triple-negative breast cancer (TNBC)/basal-like breast cancer; and second, we made a significant progress in our effort to understand the interplay between fibrosis and tumor immunity in breast cancer progression. As a result of our exciting findings, we are on track to submit two manuscripts to high-impact journals over the next six months.

Project 1: A novel mass-spectrometry method resulted in identifying lysyl hydroxylase 2 (LH2)-derived collagen cross-link in TNBC/basal-like breast cancer.

In my original proposal, I didn't plan to be a key contributor in the effort to develop cross-linked amino acid analysis method (xAAA) – I decided to co-lead this project with Alex Barrett (a graduate student in Dr. Hansen's lab) because there was a paramount need to establish a high throughput, specific, and quantitative method to measure collagen cross-links in complex biological samples such as solid tumors. In this report, we present data on how this assay could be reliably utilized to assess the fibrotic state of desmoplastic stroma and allowed us to profile collagen cross-links in human breast cancer subtypes.

Progress on project 1:

The formation of lysyl oxidase (Lox)-mediated collagen cross-links is a key driver of structural and biomechanical remodeling events associated with ECM during tumor progression. Despite the appreciation for a role of collagen cross-linking in establishing a desmoplastic stroma, we are severely limited in our ability to evaluate these cross-links in complex biological specimens, like human breast tumors. Here, we present a mass spectrometry (MS) based cross-linked amino acid analysis (xAAA) method to identify and quantify species of collagen cross-links derived from three distinct subtypes of human breast tumors, in a single assay. Interestingly, lysine aldehyde (Hyl^{ald})-derived collagen cross-links (HLCCs) were most significantly associated with ECM stiffness in basal-like breast cancer — the importance of this relationship has been further solidified by demonstrating a close correlation between high expression of lysyl hydroxylase 2 (LH2) and risk for relapse-free survival in basal-like breast cancer patients, but not luminal or HER2+.

As part of this joint effort, Dr. Hansen developed this method as described in Figure 1. We decided it would be best to validate this approach by using a novel inducible-LOX mouse model (MMTV-PyMT; Col1a1-tTA; TetO_mLox) developed in our lab under the control of Col1a1 promoter (Figure 2A). As predicted, stromal Lox overexpression resulted in accumulation of fibrillar collagen surrounding the lesions and significant increases in collagen crosslinks (Figure 2B-D) — these changes in collagen cross-linking were associated with stiffer ECM and enhanced mechanosignaling (Figure 2E, F, and H). Furthermore, we found a considerable correlation between DHLNL and Pyr cross-links and the top 10% elastic modulus values in MMTV-PyMT tumors (Figure 2G). We have recently completed a collagen cross-linking profile on a large cohort with a slight modification in the study design; we had a MMTV-PyMT;TetO_mLox (control group) and MMTV-PyMT;Col1a1-tTAd;TetO_mLox (experimental group/Lox OX) and treated the mice with DOX only between 4 and 6 weeks of age to avoid Lox overexpression during mouse female puberty. While we didn't observe a difference in a trivalent pyrrole cross-link as before, we showed that higher hydroxylysine aldehyde-derived collagen cross-links including HLNL and DHLNL (Suppl. Figure 2). These data not only demonstrated a direct positive relationship between changes in stromal Lox expression, collagen cross-linking, and tumor mechanical properties, but also making a strong case for a specific preference of LH2-derived collagen cross-links in stiffer tumor stroma.

Next, we deployed this method to profile collagen cross-links between normal breast tissue and breast cancer subtypes. First, total amount collagen cross-links significantly increased in breast tumors relative to normal breast tissue (Figure 3A-B) — this finding is consistent with previously published data from our lab where collagen linearization and ECM stiffness increase during breast cancer progression (*Acerbi et al. Integr Biol 2015*). We further investigated the role of HLCCs as there is evidence in lung adenocarcinomas that suggest LH2 is a key driver in the preference for these types of cross-links in more aggressive tumors. In fact, individual cross-linking scatter plots showed the most significant increase in HLCCs (HLNL and DHLNL) and trivalent crosslinks (e.g. Pyr) rather than LCCs (LNL) in breast tumors compared with normal breast tissues — particularly in TNBC/basal-like tumors (Figure 3C). These results suggest LH2 plays a central role in hydroxylating telopeptide lysine residues in human breast cancer tumors — especially TNBC/basal-like tumor with significant correlations between these cross-links and ECM stiffness (Figure 3D).

To further support a role for HLCC in breast cancer aggression, we evaluated whether LH2 expression correlated with relapse free survival (RFS) independent of tumor grade or treatment in a large patient cohort (Figure 4). These RFS curves unequivocally demonstrated a strong relationship between LH2 expression and poor prognosis in TNBC/basal-like breast cancer patients, but not other tumor subtypes. Taken together, these data cement a key role for LH2 in establishing a desmoplastic stroma in TNBC/basal-like breast cancer — bringing forth the notion that specific tumor subtype could have a distinct desmoplastic response.

Lastly, we are in the process to assess LH2 expression in a well-annotated large cohort of breast cancer patients (~400 specimen) via an external collaborator; we anticipate that extensive investigation of LH2 expression in specimens from breast cancer patients would allow us to determine whether LH2 is valuable biomarker for TNBC/basal-like breast cancer subtype and if this biomarker correlates with response rate to treatment or overall survival. This project is an exceptional example of how a technology can lead to actionable insight regarding a devastating disease by assessing the fibrotic state of various breast cancer subtypes.

Notice: I didn't use any of my fellowship funding to purchase or perform experiments on human specimens. My contribution includes: 1) initiating and managing the collaboration, 2) conception of the study together with our colleagues, 3) performing all animal studies and analyses, and 4) assisting with human data analyses on the cross-linking data and the LH2 staining.

Project 2: a role for fibrosis in promoting pro-tumor immunity in breast cancer

Here, I present our progress on the main project evaluating a role for fibrosis in promoting pro-tumor immunity in breast cancer progression. Last year, we have showed the ability of macrophages to promote collagen accumulation and ECM stiffness using MMTV-PyMT mouse model. These changes in tumor mechanics led to an increase in STAT3 signaling in mammary tumor cells and caused a shift in cytokine milieu toward a more pro-tumor immune response. This year I propose for the first time a putative mechanism on how macrophages alters the tumor microenvironment by augmenting STAT3 activity in mammary tumor cells and the consequences on immune cell landscape and ultimately tumor aggression.

Specific Aim 1: Examine if β1 integrin–mediated tumor cell tension increases the levels of inflammatory cytokines and degree of immunosuppression in LuBC and TNBC mouse models.

Task 1A. Generate the appropriate breeding scheme to build cohorts of tri-transgenic mice (*MMTV-PyMT; MMTV-Cre; LSL-Itgb1$^{V737N/+}$* mice and *C3(1)/Tag; MMTV-Cre; LSL-Itgb1$^{V737N/+}$* mice). The control for these studies will be *MMTV-PyMT* or *C3(1)/Tag; LSL-Itgb1$^{V737N/+}$* mice. I will start by breeding with hemizygous *MMTV-Cre; LSL- LSL-Itgb1$^{V737N/+}$* male mice with hemizygous *LSL- LSL-Itgb1$^{V737N/+}$* female mice to generate *MMTV-Cre; LSL-Itgb1$^{V737N/V737N}$* female or male mice. Then I will cross these mice with hemizygous *MMTV-PyMT* or *C3(1)/Tag* mice in the corresponding gender. These breeding scheme should result in ~12.5% female me as *MMTV-PyMT* or *C3(1)/Tag; MMTV-Cre; LSL-Itgb1$^{V737N/+}$* female mice depending on the breeding and another ~12.5% as control. *(Month 3-7)*

Task 1B. Monitor tumor growth and animal health for *MMTV-PyMT; MMTV-Cre; LSL-Itgb1$^{V737N/+}$* and control mice. FAK inhibitor treatment will begin prior to the presence of palpable tumors. *(Month 7-11)*

Task 1C. Monitor tumor growth and animal health for *C3(1)/Tag; MMTV-Cre;; LSL-Itgb1$^{V737N/+}$* mice. FAK inhibitor treatment will begin prior to the presence of palpable tumors. *(Month 7-15)*

Task 1D. Flow cytometry analyses will be performed at study endpoints using 13 different markers to characterize the immune cell profile as described in the project narrative. *(Months 11 and 15)*

Task 1E. Inflammatory cytokine analyses will be performed at study endpoints. *(Months 11 and 15)*

Task 1F. OCT-embedded and frozen mammary tumors from Task 1B and C will be used to quantify collagen deposition and organization via second harmonic generation (SHG) analysis and picro sirius red (PS) staining. Stromal stiffness will be measured using nanoindentation Atomic Force Microscopy (AFM). *(Months 11-15 for Task 1B and 15-19 for Task 1C)*

Task 1G. Immunofluorescence analyses will be done using marker for Mechanosignaling and inflammatory pathways as described in the project narrative. *(Months 11-15 for Task 1B and 15-19 for Task 1C)*

Task 1H. I will seek assistance from a trained pathologist to review histological sections to determine tumor grade and invasiveness. *(Months 11-15 for Task 1B and 15-19 for Task 1C)*

Progress on Aim 1:

Task 1A-C:
We received in the past year two novel transgenic mouse models — and we have already started the validation process or are in the final breeding stages. The first model is an inducible Lox, which was validated by: 1) detecting GFP in epithelial cells using MMTV-rtTA; TetO_mLox model (Suppl Figure 1); and 2) assessing collagen cross-linking and fibrillar collagen I deposition, and macrophage infiltration in a pilot study using MMTV-PyMT;Col1a1-tTA;TetO_mLOX model, where Lox was overexpressed in Col1a1+ stromal cells (Figure 2). The second model is an inducible LOX knockout model: MMTV-PyMT; Col1a1-CreERT;$Lox^{flx/flx}$; although the initial validation has been done with MMTV-Cre *in vivo* or Adenovirus-Cre *in vitro*. We decided to center our effort on these models for the following reasons: 1) we sought to address reviewers concerns regarding the ability of MMTV-Cre;LSL-$Itgb1^{V737N/+}$ model to enhance ECM stiffness; and 2) pursue transgenic mouse models where we directly alter mechanical properties of fibrillar collagen by increasing the amount of Lox-mediated crosslinks in tumor stroma.

Updates for current funding year (2016): none

Task 1D:
I performed an extensive flow cytometry analyses on MMTV-PyMT or C3(1)/TAg mice treated with BAPN — a small molecule LOX inhibitor — to gauge on the role of collagen crosslinking and ECM stiffness on immune cell composition. Unfortunately, the impact of BAPN treatment was unremarkable on either T cell or myeloid cell composition in MMTV-PyMT model (data not shown). Of note, a caveat of this experiment is that we don't fully understand off target effects of BAPN, especially on fast-growing tumors like MMTV-PyMT; our new transgenic models would address this concern. Nevertheless, we observed a trend toward an increase in CD8+ T cell/ T-Reg cell ratio in the BAPN group compared with control in C3(1)/TAg model (Suppl Figure 5A-B), but not MMTV-PyMT model; these data suggest ECM crosslinking may contribute to a more productive cytotoxic CD8+ T cell function in basal-like breast cancer model.

Updates for current funding year (2016):

1) We repeated the experiment of C3(1)/TAg+/- BAPN — we observed a significant increase on CD8+ T cells/T-Reg cell ratio (Suppl Figure 5C) consistent with our results from the first round. Altogether, our data suggest ECM stiffness and collagen cross-linking could influence T cell composition and potentially function in a mouse model of basal-like breast cancer.

2) We completed the RNA-seq data on TAMs sorted from MMTV-PyMT+/- BAPN. We didn't observed many transcriptional changes in relevant genes or much overlap with TAM sorted from early and later time point during tumor progression in the MMTV-PyMT model (Suppl Figure 6). Nevertheless, we obtain very exciting data regarding the changes in state of TAMs during tumor progression — TAMs at the late time point definitely upregulated genes associated with cytokines and immunosuppression compared to early time point (Figure 6C). These findings were consistent with the changes in cytokine levels like an increase in IL10 and CSF family members via ELISA like-assay (Figure 6D). Moreover, we also demonstrated changes in other myeloid populations — a decrease in MHCII high dendritic cells and an increase in neutrophils in the late time point — suggesting a shift toward a protumor immune microenvironment (Figure 6B). Finally, when we overexpressed Lox using the MMTV-PyMT;Col1a1-tTA; TetO_mLOX model, we found an increase in collagen cross-linking further augmented the trends observed in the late time point such as decreases in MHCII high APC populations and an increase in MHCII low neutrophils (Figure 6E). Similar to the late time point data, we also observed elevated levels of G-CSF and IL10 (Figure 6F). Collective, our data indicate the changes in immune landscape at least in part are driven by tissue mechanics.

Task 1E:
Our collaborator performed a preliminary cytokine array on MMTV-PyMT tumors, where they found a significant decrease IL6 and TNFα, and a trend toward an increase in IFNγ in tumors from mice treated with BAPN compared with control (data not shown). Of note, we are going to evaluate additional cytokines in order to better match our data in Aim 2. In addition, through our collaboration with Kirk Hansen, we also found that arginine levels are increased in tumors from mice treated with BAPN (data not shown), which further suggests a shift toward anti-tumor immune response. We have recently obtained enough tumors from this mouse model to perform a more extensive cytokine analysis. It would be informative to compare the changes between this model

and the inducible LOX mouse model as BAPN is currently heavily used to alter collagen cross-linking by many researchers who study fibrosis and tumor microenvironment.

Updates for current funding year (2016):

1) We performed an extensive cytokine analysis on MMTV-PyMT tumor +/- BAPN. Unfortunately, we weren't able to reproduce the trends from previous study performed by our collaborator regarding differences in IL6 and TNFα levels; these inconsistencies may be due to modifications in study design or different mouse line of MMTV-PyMT. Interestingly, we observed a significant decrease in leukemia inhibitory factor (LIF), another IL6 family member, in the BAPN group compared with control (Figure 7D right panel). These results were in accordance with a decrease in STAT3 phosphorylation in mammary tumor cells (Figure 7A bottom panel). Moreover, we demonstrated an increase in LIF levels during tumor progression, but not IL6 (Figure 7D left panel) — and an increase STAT3 phosphorylation in mammary tumor cells (Figure 7A top panel). Altogether, these data support a role for LIF, not IL6, in stimulating STAT3 phosphorylation. Finally, RNA-seq data on TAMs sorted from early and late time points in tumor progression suggesting TAMs may be the source for LIF as its expression was upregulated over three fold in the late time point (Figure 6C).

2) We are interested in identifying the main source of LIF in mammary tumor. In order to accomplish this task, we are planning to focus on three different cell populations: TAMs, cancer-associated fibroblasts (CAF), and mammary tumor cells. I will use polyacrylamide gels coated with fibronectin to tune matrix stiffness to assess LIF expression at the transcriptional level in the cells and protein levels in the conditioned media. We also will use conditioned media from each arm to evaluate if these media stimulates STAT3 phosphorylation and whether matrix stiffness further promotes its activity in mammary tumor cells. In fact, we have previously showed matrix stiffening promotes STAT3 phosphorylation (Figure 7B); we expect stiffer matrix and conditioned media from TAMs would result in significantly higher levels of STAT3 phosphorylation compared with each condition alone.

Task 1F:
We have already published that BAPN treatment alters ECM stiffness, collagen deposition and organization in MMTV-PyMT tumors. In addition, I found BAPN significantly reduces ECM stiffness and for a lesser degree collagen deposition in C3(1)/TAg tumors (see Aim 3).

Updates for current funding year (2016):

1) We demonstrated stromal Lox overexpression in the inducible LOX mouse model caused an increase in ECM stiffness and enhanced mechanosignaling in a small cohort of mice. We are now in the midst of expanding this cohort (Suppl Figure 2).

Task 1G:
Updates for current funding year (2016):

1) Same as Task 1F

Task 1H:
In progress

Specific Aim 2: Determine whether constitutively active STAT3 in mammary tumor cells increases invasiveness by promoting immune evasion, enhancing cellular contractility and ECM stiffness.

Task 2A. Generate the appropriate breeding scheme to build cohorts of tri-transgenic mice (*MMTV-PyMT; Stat3$^{C/+}$* mice and *C3(1)/Tag; Stat3$^{C/+}$* mice). The control for these studies will be *MMTV-PyMT* or *C3(1)/Tag; Stat3$^{+/+}$* mice. I can try to generate homozygous *Stat3$^{C/C}$* mice; however these mice die within 4 months. These breeding scheme should result in ~12.5% female me as *MMTV-PyMT* or *C3(1)/Tag; Stat3$^{C/+}$* female mice depending on the breeding and another ~12.5% as control. *(Month 7-11)*

Task 2B. Monitor tumor growth and animal health for *MMTV-PyMT; Stat3$^{C/+}$* and control mice. FAK inhibitor treatment will begin prior to the presence of palpable tumors. *(Month 11-15)*

Task 2C. Monitor tumor growth and animal health for *C3(1)/Tag; Stat3$^{C/+}$* mice. The β-aminopropionitrile inhibitor treatment will begin prior to the presence of palpable tumors. *(Month 11-19)*

Task 2D. Same as Task 1D. *(Months 15 and 19)*

Task 2E. Inflammatory cytokine analyses will be performed at study endpoints. *(Months 15 and 19)*

Task 2F. Same as Task 1F. *(Months 15-19 for Task 2B and 19-23 for Task 2C)*

Task 2G. Same as Task 1G. *(Months 15-19 for Task 2B and 19-23 for Task 2C)*

Task 2H. Same as Task 1H. *(Months 15-19 for Task 2B and 19-23 for Task 2C)*

Task 2I. Proposed *in vitro* studies will be completed as described in the project narrative. *(Months 15-23)*

Progress on Aim 2:

Task 2A:
We decided to work with the conditional STAT3 knockout model because it would be difficult to discern the function of each cellular compartment in the constitutively active STAT3 model, where all tumor, stromal, and immune cells have higher levels of STAT3 activity. We focus on STAT3 activity in epithelial cells because: 1) we aim to understand how tumor cells and tissue mechanics influence cytokine milieu; 2) a role for STAT3 activity in tumor-initiating cells (TICs) is well-known in mouse models of breast cancer; and 3) we have evidence that there is a direct correlation between TIC expansion (CD24 high CD29 pos) and alterations in immune cell composition consistent with pro-tumor immune response during mammary tumor progression (data not shown).

I completed multiple studies with *MMTV-PyMT; MMTV-Cre; Stat3$^{flx/flx}$* model to assess the effects of epithelial STAT3 on cytokine milieu and fibrosis in mammary tumors. Consistently with previously published data, we observed a significant decrease in metastatic incidence in the STAT3 KO group compared with control (Figure Suppl. Figure 7B).

Task 2B-C:
Completed for MMTV-PyMT model. I found no difference in tumor growth when STAT3 knocked out in epithelial cells (data not shown). I didn't perform any studies yet looking on the effects of FAK inhibitor or BAPN treatment.

Task 2D:
Updates for current funding year (2016):

1) We completed an immune cell profile on mammary tumors from *MMTV-PyMT; MMTV-Cre; Stat3$^{flx/flx}$* models. Our findings were consistent with data presented in a similar model from *Jones et al. Cancer research 2016* with a few additions. Briefly, mammary tumors from the STAT3 KO mice had a decrease in the number of neutrophils, increases in CD103 DC/CD11b DC ratio and MHCII high monocytes, and no change in TAMs compared to control as a percentage of CD45 cells (Figure 8D and Suppl. Figure 7C). We also observed an increase in the number of total CD45 and an upward trend in CD3 T cells in STAT3 KO tumors as a percentage of live cells (Suppl Figure 7D,E). Collectively, these data further support a role for epithelial STAT3 activity in promoting a protumor immune environment.

Task 2E:
Completed for MMTV-PyMT model. I found a shift in cytokine milieu in whole mammary tissue homogenates from STAT3 KO mice compared with control consistent with anti-tumor immune response (Figure 8E).

Task 2F:
Completed for MMTV-PyMT model. I found a decrease in ECM stiffness and fibrillar collagen deposition in the STAT3 KO group compared with control (Figure 8A-B).

Task 2G:

In progress. I observed a decrease in phospho-SMAD2 Ser465/Ser467 in stromal cells adjacent to MMTV-PyMT tumors in mice, where STAT3 was knocked out in epithelial cells (Suppl. Figure 8A). This is consistent with our data showing a decrease in ECM stiffness and a reduction in TGFβ levels in the STAT3 KO group in mice (Suppl. Figure 8B). Thus, I am currently evaluating impact of TGFβ and ECM stiffness on macrophage polarization using polyacrylamide gels and co-culture models.

Updates for current funding year (2016):

1) I were finally able to optimize anti-active TGFβ antibody and I am planning to co-stain with F4-80 and pSMAD2 Ser465/Ser467 in tumor from the STAT3 KO model to better define the contribution TGFβ to macrophage differentiation.

2) In the meantime, we are currently evaluating on whether TGFβ signaling in macrophage cooperates with collagen I stiffness to promote metastatic disease using an orthotopic syngeneic model. We used non-enzymatic glycation to enhance collagen I stiffness prior to mixing it with MMTV-PyMT cells and injecting to clear mammary fat pad.

Task 2H:
In progress

Specific Aim 3: Test if anti-fibrotic treatment reduces mechanosignaling and STAT3 activity, while potentiating the effects of immunotherapy to impede metastatic disease.

Task 3A. I will treat C3(1)/Tag mice and MMTV-PyMT with low dosage simvastatin starting at 2 months and 4 weeks, respectively. Spontaneous tumor models are more similar to the human condition and allow us to better assess how treatment influences immunity and disease progression. *(Months 3-10)*

I will need a total of 10 mice for each group per model to assess whether simvastatin induces changes in tumor immunity and tissue tension.

In addition, if needed, I will inject tumor cell lines using an orthotopic syngeneic model. This approach will allow us to take a mechanistic approach and determine functions of specific signaling modulators (STAT3 or β1 integrin mutant). This approach will involve isolating mammary tumor cells from C3(1)/Tag and MMTV-PyMT mouse model. I will prepare several cell lines where I manipulate β1 integrin and/or STAT3. I will generate derivative 4 cell lines for each original cell line (MMTV-PyMT (obtained from Dr. Werb's lab, UCSF) and C3(1)/Tag): 1) β1 integrin mutant overexpression and STAT3 knockdown; 2) Constitutively active STAT3 overexpression and β1 integrin knockdown; 3) β1 integrin mutant and constitutively active STAT3 overexpression; 4) β1 integrin mutant and constitutively active STAT3 knockdown. Inject tumor cell lines into the 4th mammary gland and monitor tumor growth and metastatic incidence. *(Months 10-15)*

I will need a total of 5-10 mice for each group per model to assess whether a specific signaling modulator induces changes in tumor immunity and tissue tension. If variations within specific groups will be greater than expected, I may need to increase the number of animals.

Task 3B. Same as Task 1D.

Task 3C. Same as Task 1E.

Task 3D. Same as Task 1F.

Task 3E. Same as Task 1G.

Task 3F. Monitor tumor cell invasion and contractility in collagen gels in the presence of simvastatin using the tumor cell lines described in Task 3A. *(Months 5-7)*

Task 3G. Same as Task 1A if I decided to use transgenic mouse model (1st choice). Otherwise, I will use orthotopic model using tumor cell lines generated in 3A. *(Months 23-31)*

Task 3H. Monitor tumor growth and animal health. Simvastatin treatment will start prior to the presence of palpable tumors. Short-term treatment with chemotherapeutic (alone) or immunotherapeutic agent (in combination with simvastatin) will be initiated when control mice are expected to have malignant disease.

Task 3I. Same as Task 1D.

Task 3K. Same as Task 1E.

Task 3L. Same as Task 1F.

Task 3M. Same as Task 1G.

Progress on Aim 3:

Task 3A:
In progress. I isolated primary mammary tumor cells from C3(1)/TAg model; however, these cell lines didn't form tumors when injected to syngeneic FVB/n strain female mice. I will need to further different component in medium and characterize the isolated cells to make sure I don't select for a subpopulation of tumor cells with low tumorigenicity. In the meantime, I decide to focus on testing the effects of simvastatin treatment on tumors in the C3(1)/TAg model (transgenic, not orthotopic). I am also at the final stages of obtaining several breeding pairs for: C3(1)/TAg; MMTV-Cre; LSL-Itgb1$^{V737N/\ V737N}$ mice.

Task 3B:
In progress. I isolated primary tumor organoids from C3(1)/TAg model and embedded in collagen I gels. The primary tumor organoids didn't adapt to these collagen gels as the PyMT organoids using the same defined media. We are trying to figure out these cell culture issues with isolated cells from C3(1)/TAg model.

Task 3C-E:
In progress. Interestingly, I found that mammary tumors in C3(1)/TAg are more fibrotic and have higher number of αSMA+ cancer-associated fibroblasts compared with MMTV-PyMT (Suppl. Figure 9) — similar to work we have recently published, where basal-like tumors are more fibrotic relative to luminal B. To begin addressing the effect of simvastatin on tissue fibrosis in mammary tumorigenesis, I treated mice with BAPN, low or high dosage of simvastatin in C3(1)/TAg model — I determined clinically-relevant dosages of simvastatin by using FDA-recommended conversion factor from human to mice. I observed significantly smaller tumors in mice treated with high dose of simvastatin compared to control (Suppl. Figure 10B). Moreover, high dose simvastatin treatment decreased levels of phospho-FAK Y397 and ECM stiffness (Suppl. Figure 10C), but quantitative analyses would be necessary to determine differences in fibrillar collagen deposition and aSMA+ fibroblasts. This reduction in mechanosignaling significantly correlated with a decrease in ECM stiffness (Suppl. Figure 10D).

Once we have enough breeding pairs, I will use C3(1)/TAg; MMTV-Cre; LSL-Itgb1$^{V737N/\ V737N}$ mice to determine if enhanced integrin signaling in tumor cells increases metastatic incidence as it is usually very low in C3(1)/TAg (only ~10% of mice). I will also have an arm with high dose simvastatin treatment.

Updates for current funding year (2016):

1) We repeated the C3(1)/TAg+/- BAPN or high dose simvastatin and we are currently analyzing the data.

2) We finally have breeding pairs for C3(1)/TAg;MMTV-Cre; LSL-Itgb1$^{V737N/\ V737N}$ — it took us longer than expected to establish a colony due to the complexity of the breeding and a few setbacks.

Task 3F:
In progress.

Task 3G-K:
I identified a meaningful increase in CD103+ DC — this population is known to be a potent inducer of CD8+ T cell activity — in mammary tumors of mice treated with high dose of simvastatin (Suppl Figure 11C); however, such an increase was not observed with mice treated with BAPN due high variance among tumors in this group. We suspect that the simvastatin impedes tumor cell contractility as suggested by the phospho-FAK Y397 staining — and it induces changes in ECM stiffness and possibly cytokine milieu. To test this hypothesis, we are generating C3(1)/TAg; MMTV-Cre; LSL-Itgb1$^{V737N/\ V737N}$ model and I will proceed with these tasks in this model. Of note, in future experiment, we will use a myeloid panel that would better discern among myeloid population as propose in Suppl. Figure 3.

Updates for current funding year (2016):

1) We repeated the C3(1)/TAg+/- BAPN or high dose simvastatin and we are currently analyzing the data.

Figure Legends:

Figure 1. ***Schematic diagram of collagen cross-linking and overview of xAAA method.*** (**A**) Lysyl hydroxylase 2 (LH2) hydroxylates telopeptide lysine resides on procollagen prior to formation of mature collagen through cleavage by procollagen N- and C-endopeptidases. Following cleavage mature collagen undergoes the final step in biosynthesis — intermolecular cross-linking (**B**) Lysyl oxidase (LOX) modifies telopeptide and helix lysine and hydroxylysine residues to form lysine aldehyde Lys^{ald} and hydroxylysine aldehyde Hyl^{ald}, respectively. Aldehyde modified lysine will react through aldol condensation reactions to form immature (divalent) cross-links between two mature collagen fibers. (**C**) Following surgical resection, OCT-embedding and storage in a biobank, prophylactic breast tissues or breast tumor biopsies undergo hydrolysis and enrichment prior to LC-MS/MS analysis using full MS and parallel reaction monitoring (PRM) modes. Quantification is performed by comparing the peak areas of a given cross-link between prophylactic and tumor tissue specimens after normalization to hydroxyproline content and starting tissue weight.

Figure 2. ***Collagen cross-linking closely correlates with fibrillar collagen abundance and ECM stiffness in a mouse tumor model.*** **(A)** Lysyl oxidase (Lox) expression was induced under the control of the Col1a1 promoter using a TetOFF system when MMTV-PyMT mice were taken off doxycycline treatment at 6 weeks of age. (**B**) Picrosirius Red staining and imaging of doxycycline treated mice with MMTV-PyMT tumors (Control) or mice on water where stromal Lox was overexpressed (Lox OX). (**C**) Quantification of total cross-links between two tumor groups. Cross-links were summed for each animal and averages plotted with standard error of the mean (SEM) ($P < 0.05$). (**D**) Comparison of normalized peak areas of individual cross-links in tumor hydrolysates. Each point represents an animal with horizontal and vertical bars representing the mean and SEM, respectively (*p< 0.05). The horizontal lines represents the means (***P<0.0001). (**E-F**) AFM used to measure ECM stiffness in control and Lox OX tumors coupled with second harmonic generation (SHG) imaging via two-photon microscopy to assess fibrillar collagen presence and architecture at the same regions. (**G**) A correlation map between collagen cross-links and top 10% elastic modulus values. (**H**) Representative images of phosphor-FAK Y397 via immunofluorescence. All statistical analyses were performed using unpaired two-tailed Student's t-tests.

Figure 3. ***Human basal-like breast cancer features a distinct hydroxylysine collagen cross-link.*** (**A**) Quantification of total cross-links between normal (prophylactic) tissue and tumor independent of subtype. (**B**) Plot of total cross-links among various human breast cancer subtypes (ANOVA *P < 0.05). (**C**) Scatterplots for individual cross-links identified from prophylactic breast tissue and breast tumor subtypes (ANOVA with Tukey's method for multiple comparisons ** P < 0.01). * denotes significance relative to normal unless denoted by a horizontal bar specifically comparing two groups (*P < 0.05, ** P < 0.01). (**D**) Correlation maps display the relationships between ECM stiffness, collagen I content and individual crosslinks.

Figure 4. ***High LH2 expression correlates with poorer prognosis in triple-negative breast cancer patients, but not other breast cancer subtypes.*** Plots assess the relationship between LH2 expression and relapse free survival in ER+/PR+ (luminal), HER+ and basal-like (ER-/PR-/HER2-) breast tumors. Gene expression data were obtain from *Szasz AM et al. Oncotarget. 2016.* DOI: 10.18632/oncotarget.

Figure 5. Early macrophage depletion attenuates fibrosis and ECM stiffness in mammary tumors. (**A**) A correlation plot between CD14hi CD11b+ HLA-DA+ TAM and ECM stiffness in human breast cancer. (**B**) MMTV-PyMT female mice were treated with IgG control or anti-CSF1-neutralizing antibody i.p. delivered starting at 4 weeks of age. Mice were euthanized at 11 weeks of age. Bottom panel: representative images of phospho-FAK Y397 via IF. (**C**) Fibrillar collagen architecture and deposition were assessed via 2-photon/ second harmonic generation imaging and picrosirus red staining. N=5-6 mice per group. (**D**) ECM stiffness adjacent to MMTV-PyMT tumors has been evaluated via atomic force microscopy (AFM). N=4-5 mice per group and at least two force maps per sample. (**E**) Lung metastases were detected by measuring PyMT transcript via qPCR. Statistical analysis performed using unpaired Student's t-test.

Figure 6. ***Fibrosis promotes a protumor immune response during mammary tumor progression.*** (**A**) Fibrillar collagen architecture and deposition were assessed in mammary tumors at early (8-9 weeks of age) and late time point (11-12 weeks of age) in FVB/n MMTV-PyMT mouse model via picrosirus red staining. (**B**) Immune cell landscape were determined via multicolor flow cytometry (FC). (**C**) MHCII high TAMs were sorted and RNA was extracted for RNA-seq analysis. N=3 and we performed RawP and FDR statistical analyses to identify

significant transcriptional changes in MHCII hi TAM between early and later time points. (**D**) Cytokine milieu has been evaluated in tissue homogenates of mammary tumors using Multiplexing LASER Bead Technology by Eve technology. Samples were normalized to protein concentration of tissue homogenates via BCA. (**E**) Similar to 6B. (**F**) Similar to 6D. Statistical analysis performed using unpaired Student's t-test unless stated otherwise.

Figure 7. ***Tissue mechanics enhances LIF-dependent STAT phosphorylation in tumor cells.*** (**A**) phospho-STAT3 Y705, pan cytokeratin (5, 8 and 18) has been assessed via IF in three MMTV-PyMT models: 1) early and late time point, 2) MMTV-PyMT; TetO_mLox (control) and MMTV-PyMT; Col1a1-tTA; TetO_mLOX, and 3) MMTV-PyMT +/-Lox inhibitor (BAPN treatment). (**B**) Representative images of STAT3 pY705 was evaluated in mammary tumor cell line (MET1) when cultured on polyacrylamide gels in various stiffness levels via immunoblotting. We used 1μM PND-1186 to inhibit FAK activity. (**C**) IL6 and LIF have been evaluated as described in Figure 6D. Statistical analysis performed using unpaired Student's t-test.

Figure 8. ***STAT3 ablation in mammary tumor cells results in a decrease in fibrotic phenotype and a shift toward anti-tumor immune response.*** (**A**) Fibrillar collagen architecture and deposition were assessed via 2-photon/ second harmonic generation imaging and picrosirus red staining. (**B**) ECM stiffness adjacent to MMTV-PyMT tumors has been evaluated via AFM. (**C**) The covalent pyridinium cross-link pyridinoline levels have been measured via xAAA method described in Figure 1. Cytokine milieu has been evaluated using the same approach as in Figure 6D. Statistical analysis performed using unpaired Student's t-test.

Figure 9. ***A putative model for a role for fibrosis in driving protumor immune response during mammary tumor progression.***

Supplemental Figures:

Suppl. Figure 1. ***Proof-of-concept experiment to validate tet-inducible lysyl oxidase transgenic mouse.*** MMTV-rtTA; TetO_mLOX mice have been treated with 2 mg/mL doxycycline plus 5% sucrose starting 6 weeks of age. Tumor cells were isolated and analyzed using FC.

Suppl Figure 2. Stromal Lox enhances abundance of HLCC in mammary tumors. MMTV-PyMT; TetO_Lox (control) and MMTV-PyMT; Col1a1-tTA; TetO_mLox (Lox OX) mice have been treated with 2 mg/mL doxycycline plus 5% sucrose from 4 to 6 weeks of age and then with 5% sucrose only until the end of the study.

Suppl Figure 3. ***Gating strategy for myeloid populations.***

Suppl Figure 4. ***Gating strategy for T cell populations.***

Suppl Figure 5. ***Lox inhibition altered T cell composition in mouse of model of basal-like breast cancer.*** (**A**) Gating strategy to identify various T cell populations. (**B**, **C**) The ratio of CD8+ T cells and FoxP3+ T regulatory cells in the first and second cohort of mice were assessed via FC, respectively. Statistical analysis performed using unpaired Student's t-test.

Suppl. Figure 6. ***Transcriptional changes in MHCII high TAM from MMTV-PyMT tumors.***

Suppl. Figure 7. ***STAT3 ablation in tumor cells alter immune cell composition toward anti-tumor immune response.*** (**A**) STAT3 pY705 was evaluated in tumors from MMTV-PyMT mice to confirm STAT3 knockout in epithelial cells via IF. (**B**) Lung metastases were detected using qPCR on RNA from whole-tissue homogenates. Statistical analysis performed using unpaired Student's t-test. (**C**) Dendritic cell populations were assessed as a percentage of CD45 via FC. (**D**, **E**) CD3 T cells and CD45 were assessed as a percentage of live cells via FC. Statistical analysis performed using unpaired Student's t-test.

Suppl. Figure 8. ***STAT3 activity in tumor cells enhances TGFβ signaling in tumor stroma.*** (**A**) Representative images of cytokeratin and phospho-SMAD2 Ser465/467 staining in MMTV-PyMT tumor via IF. (**B**) TGFβ levels from tissue homogenates of mammary tumors from control and STAT KO groups were measured as described in Figure 6D. (**C**) Mammary tumor organoids were isolated and embedded in stiff collagen gels (~4 kPa) and conditioned media were used to assess TGFβ levels.

Suppl. Figure 9. ***C3(1)/Tag — mouse model of basal-like breast cancer— is significantly more fibrotic than MMTV-PyMT.*** Representative images of picrosirus red and αSMA staining. Scale bars, 100μm

Suppl. Figure 10. ***High-dosage of simvastatin treatment hampers tumor growth rate and reduces FAK phosphorylation.*** (**A**) Schematic of study design. (**B**)Tumors were measured bi-weekly and growth rates were calculated by fitting a straight line among measurements. Statistical analysis performed using one-way ANOVA with Kruskal-Wallis test to assess overall significance (*$p<0.05$) and an unpaired Student's t-test to assess the relationship between control group and high-dose simvastatin group. (**C**) Representative images of picro-sirus red, αSMA and phosphor-FAK Y397 staining. Scale bars, 100μm. (**D**) ECM stiffness adjacent to C3(1)/TAg tumors has been evaluated via AFM. Statistical analysis performed using unpaired two-tailed Student's t-test.

Suppl. Figure 11. ***Simvastatin treatment enhances CD103+ dendritic cell infiltration and thus may contribute to anti-tumor immune response.*** (**A**-**C**) Flow cytometric data of dendritic cell (DC) populations found in C3(1)/TAg tumors. (**D**, **E**) Flow cytometric data of T cell populations and a ratio of CD8+ T cells and FoxP3+ T regulatory cells, respectively.

Figures:

Figure 1

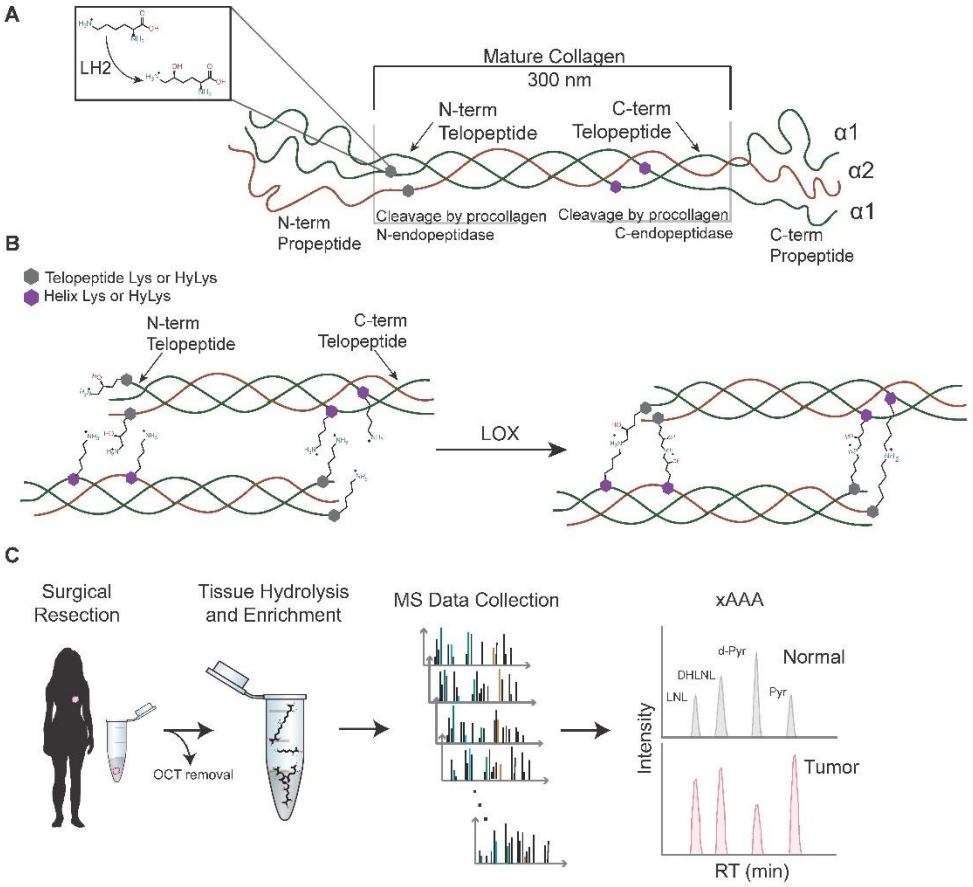

Figure 2

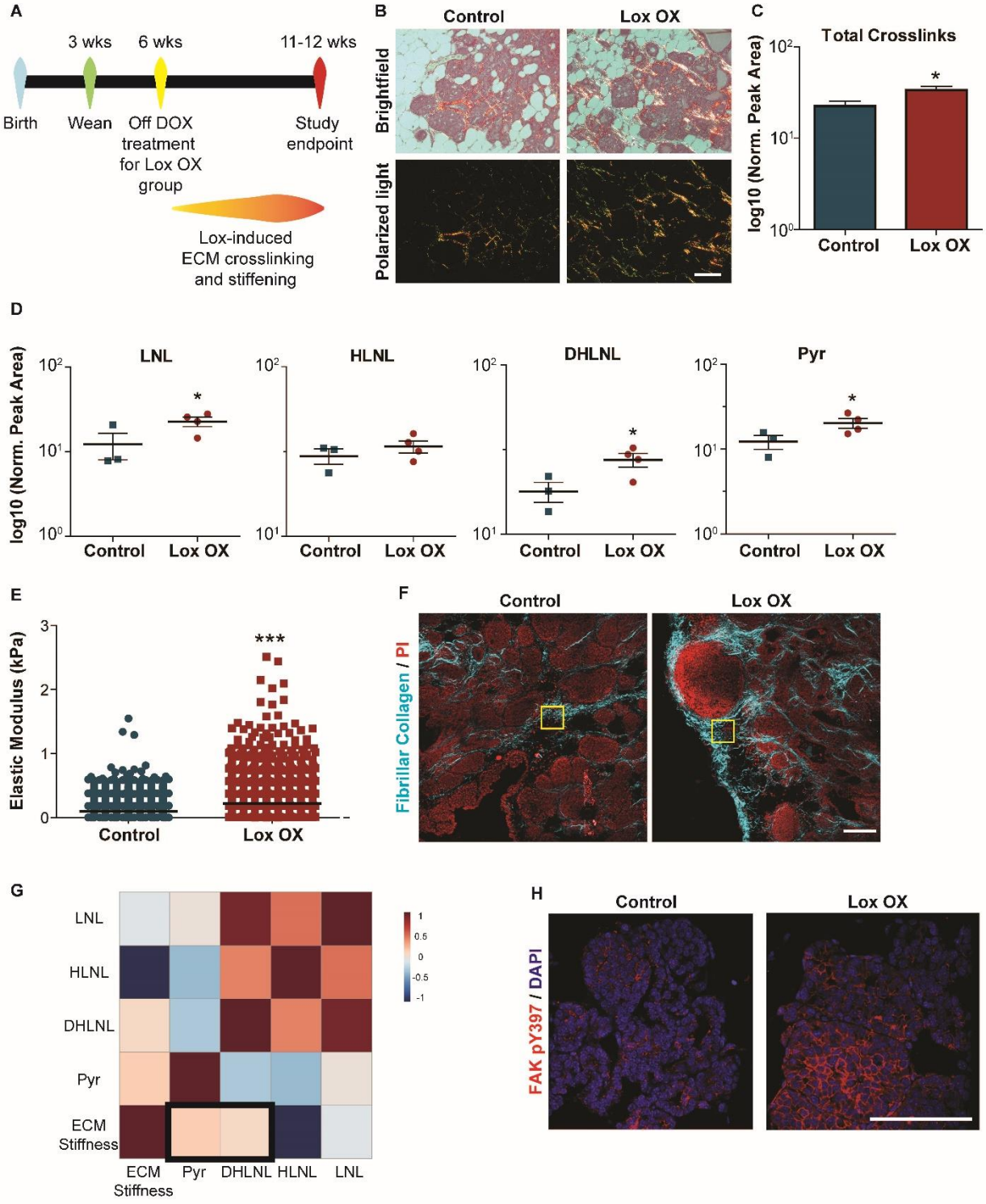
A
3 wks
6 wks
11-12 wks
Birth
Wean
Off DOX treatment for Lox OX group
Study endpoint
Lox-induced ECM crosslinking and stiffening
B
Control
Lox OX
Brightfield
Polarized light
C
Total Crosslinks
log10 (Norm. Peak Area)
Control
Lox OX
D
LNL
HLNL
DHLNL
Pyr
log10 (Norm. Peak Area)
Control
Lox OX
E
Elastic Modulus (kPa)
***
Control
Lox OX
F
Control
Lox OX
Fibrillar Collagen / PI
G
LNL
HLNL
DHLNL
Pyr
ECM Stiffness
ECM Stiffness
Pyr
DHLNL
HLNL
LNL
1
0.5
0
-0.5
-1
H
Control
Lox OX
FAK pY397 / DAPI

Figure 3

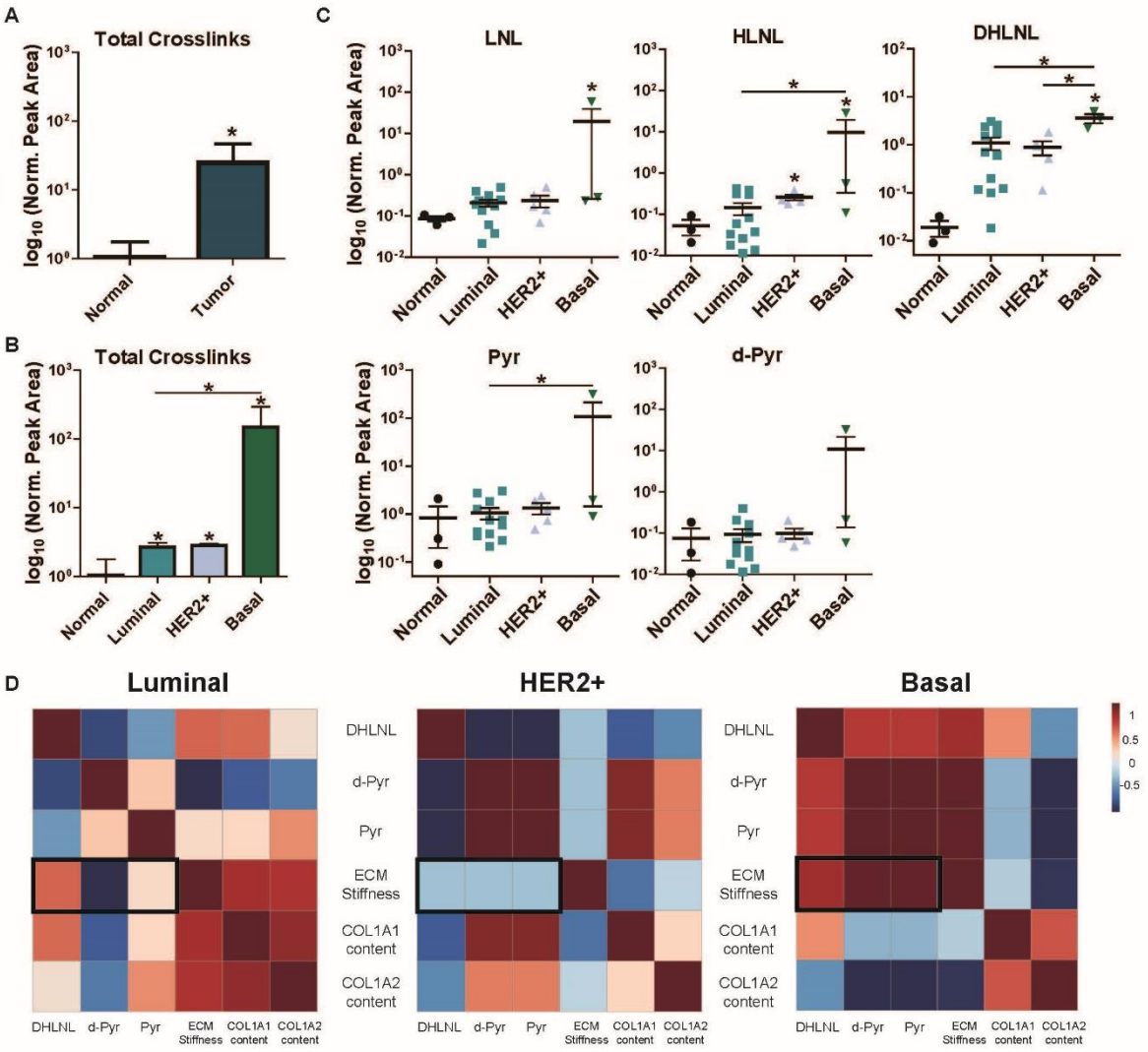
A
Total Crosslinks
log10 (Norm. Peak Area)
Normal
Tumor
B
Total Crosslinks
log10 (Norm. Peak Area)
Normal
Luminal
HER2+
Basal
C
LNL
HLNL
DHLNL
Pyr
d-Pyr
D
Luminal
HER2+
Basal
DHLNL
d-Pyr
Pyr
ECM Stiffness
COL1A1 content
COL1A2 content
1
0.5
0
-0.5

Figure 4

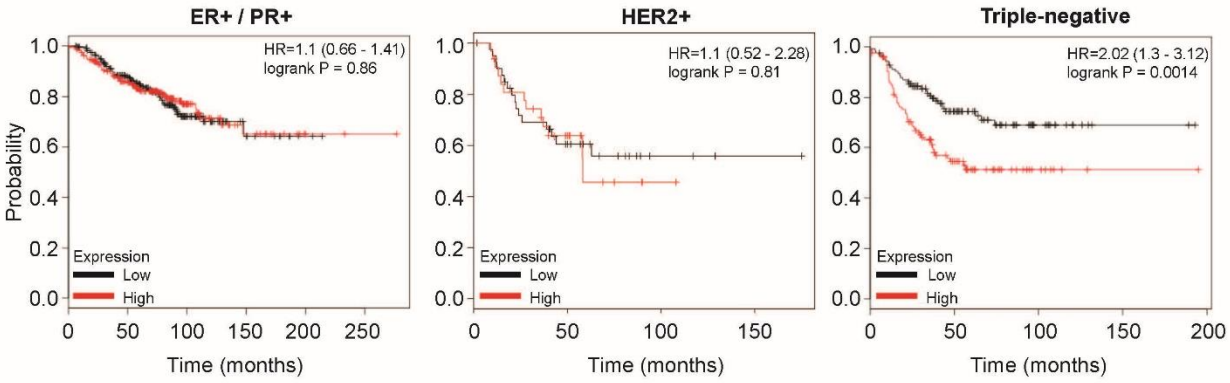
ER+ / PR+
HR=1.1 (0.66 - 1.41)
logrank P = 0.86
HER2+
HR=1.1 (0.52 - 2.28)
logrank P = 0.81
Triple-negative
HR=2.02 (1.3 - 3.12)
logrank P = 0.0014
Probability
Expression
Low
High
Time (months)

Figure 5

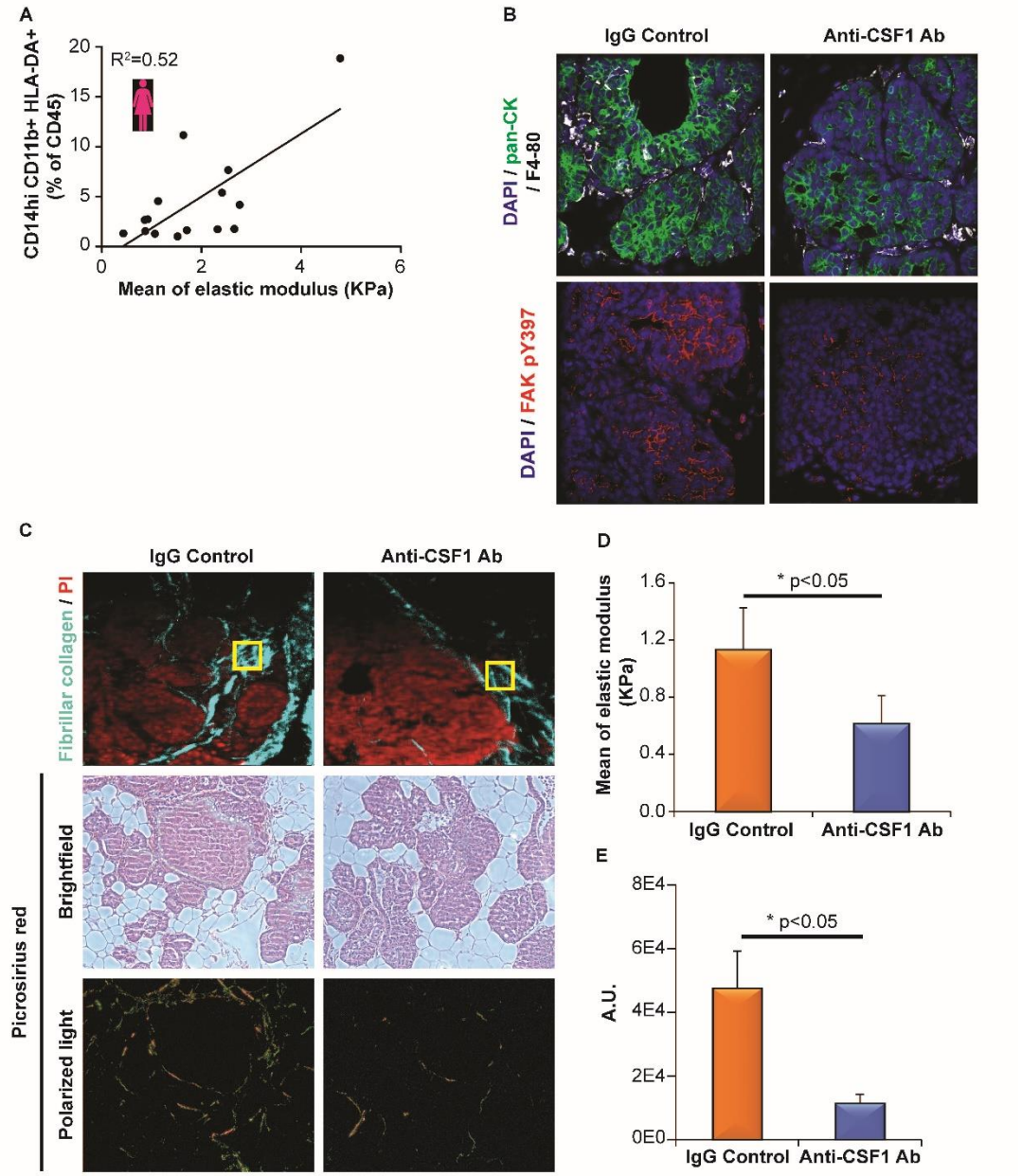
A
CD14hi CD11b+ HLA-DA+ (% of CD45)
R²=0.52
Mean of elastic modulus (KPa)
B
IgG Control
Anti-CSF1 Ab
DAPI / pan-CK / F4-80
DAPI / FAK pY397
C
IgG Control
Anti-CSF1 Ab
Fibrillar collagen / PI
Picrosirius red
Brightfield
Polarized light
D
Mean of elastic modulus (KPa)
* p<0.05
IgG Control
Anti-CSF1 Ab
E
A.U.
* p<0.05
IgG Control
Anti-CSF1 Ab

Figure 6

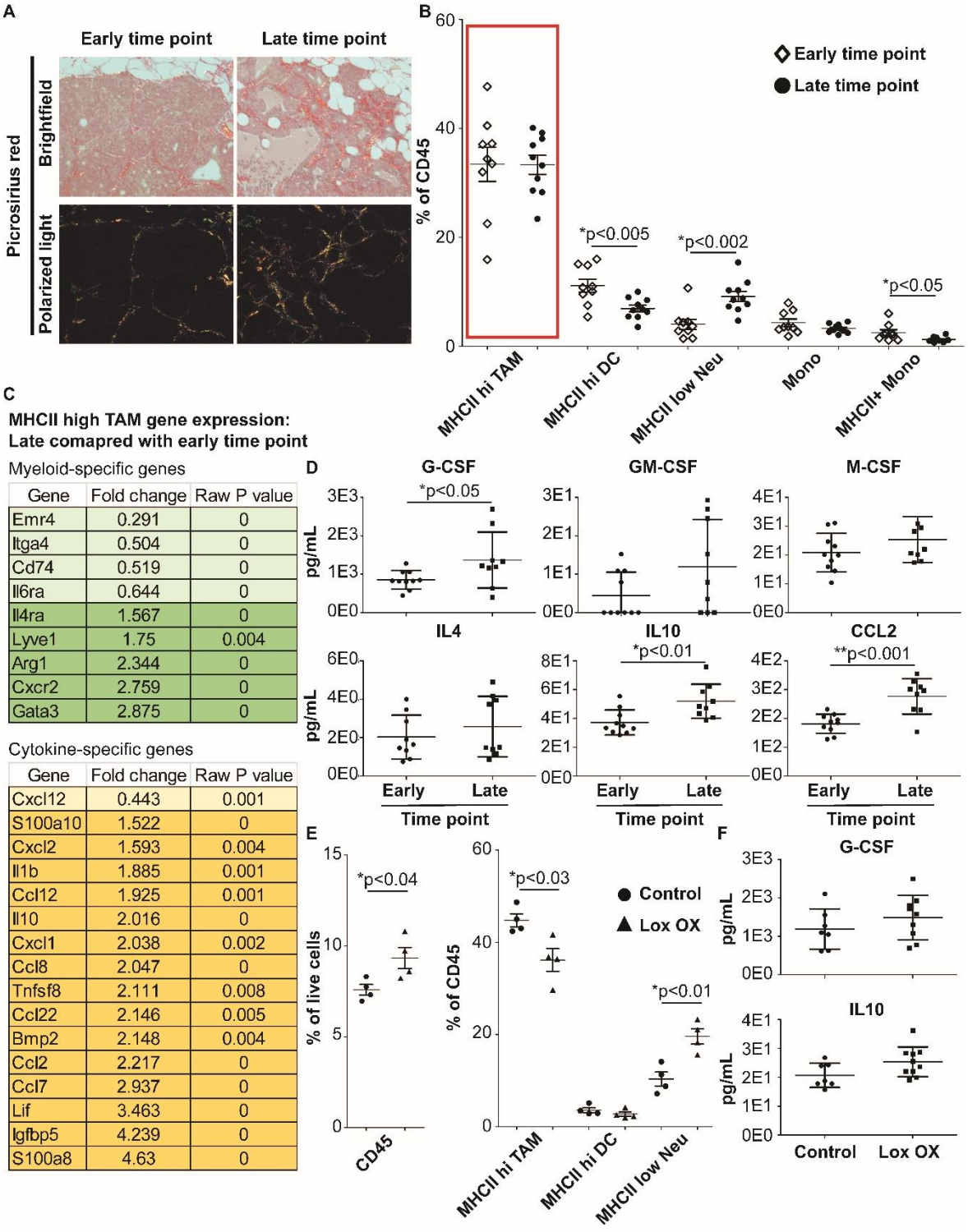

Gene	Fold change	Raw P value
Emr4	0.291	0
Itga4	0.504	0
Cd74	0.519	0
Il6ra	0.644	0
Il4ra	1.567	0
Lyve1	1.75	0.004
Arg1	2.344	0
Cxcr2	2.759	0
Gata3	2.875	0

Gene	Fold change	Raw P value
Cxcl12	0.443	0.001
S100a10	1.522	0
Cxcl2	1.593	0.004
Il1b	1.885	0.001
Ccl12	1.925	0.001
Il10	2.016	0
Cxcl1	2.038	0.002
Ccl8	2.047	0
Tnfsf8	2.111	0.008
Ccl22	2.146	0.005
Bmp2	2.148	0.004
Ccl2	2.217	0
Ccl7	2.937	0
Lif	3.463	0
Igfbp5	4.239	0
S100a8	4.63	0

Figure 7

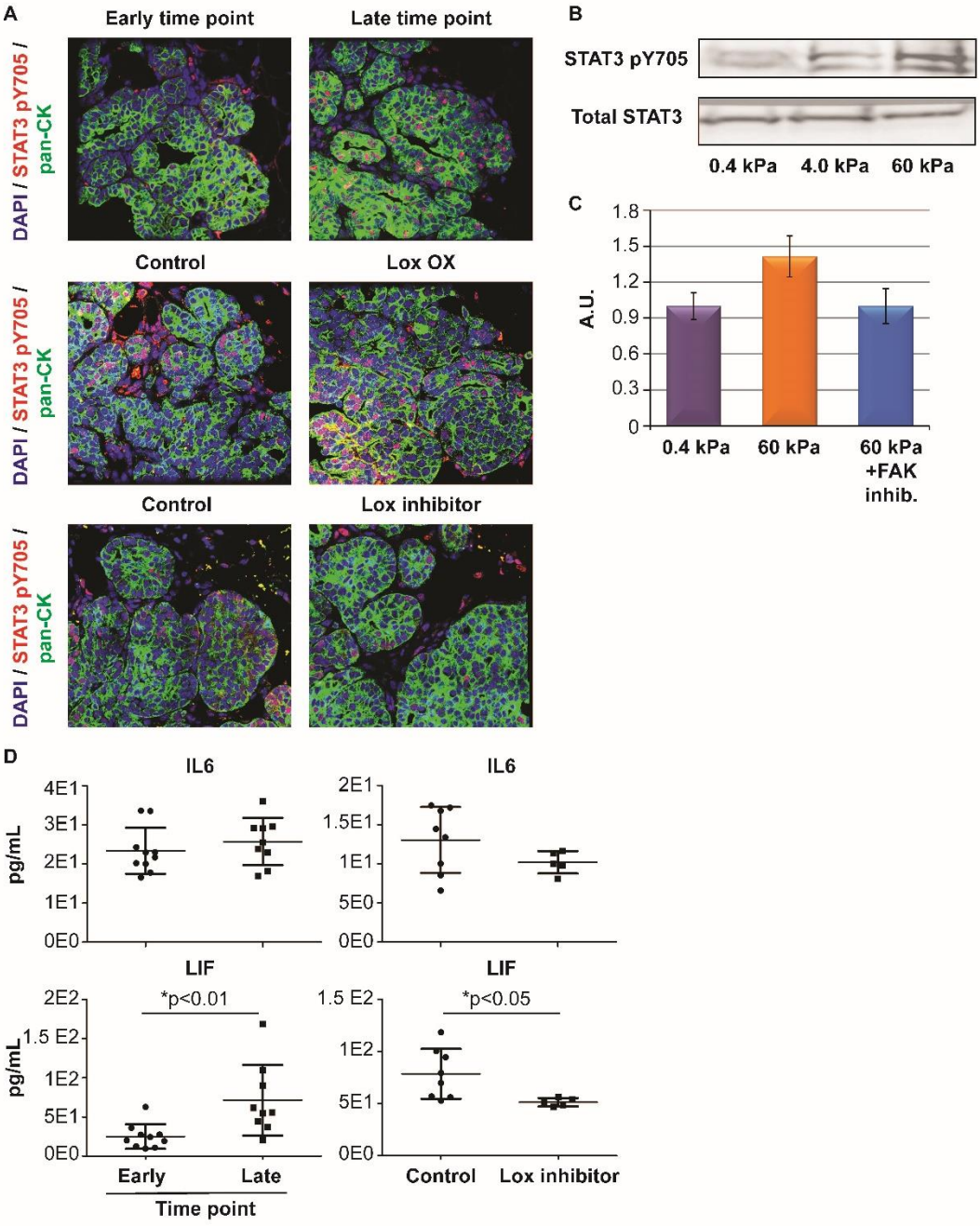
A
Early time point
Late time point
DAPI / STAT3 pY705 / pan-CK
Control
Lox OX
Control
Lox inhibitor
B
STAT3 pY705
Total STAT3
0.4 kPa
4.0 kPa
60 kPa
C
A.U.
1.8
1.5
1.2
0.9
0.6
0.3
0
0.4 kPa
60 kPa
60 kPa +FAK inhib.
D
IL6
pg/mL
4E1
3E1
2E1
1E1
0E0
2E1
1.5E1
1E1
5E0
0E0
LIF
2E2
1.5 E2
1E2
5E1
0E0
*p<0.01
*p<0.05
Early
Late
Time point
Control
Lox inhibitor

Figure 8

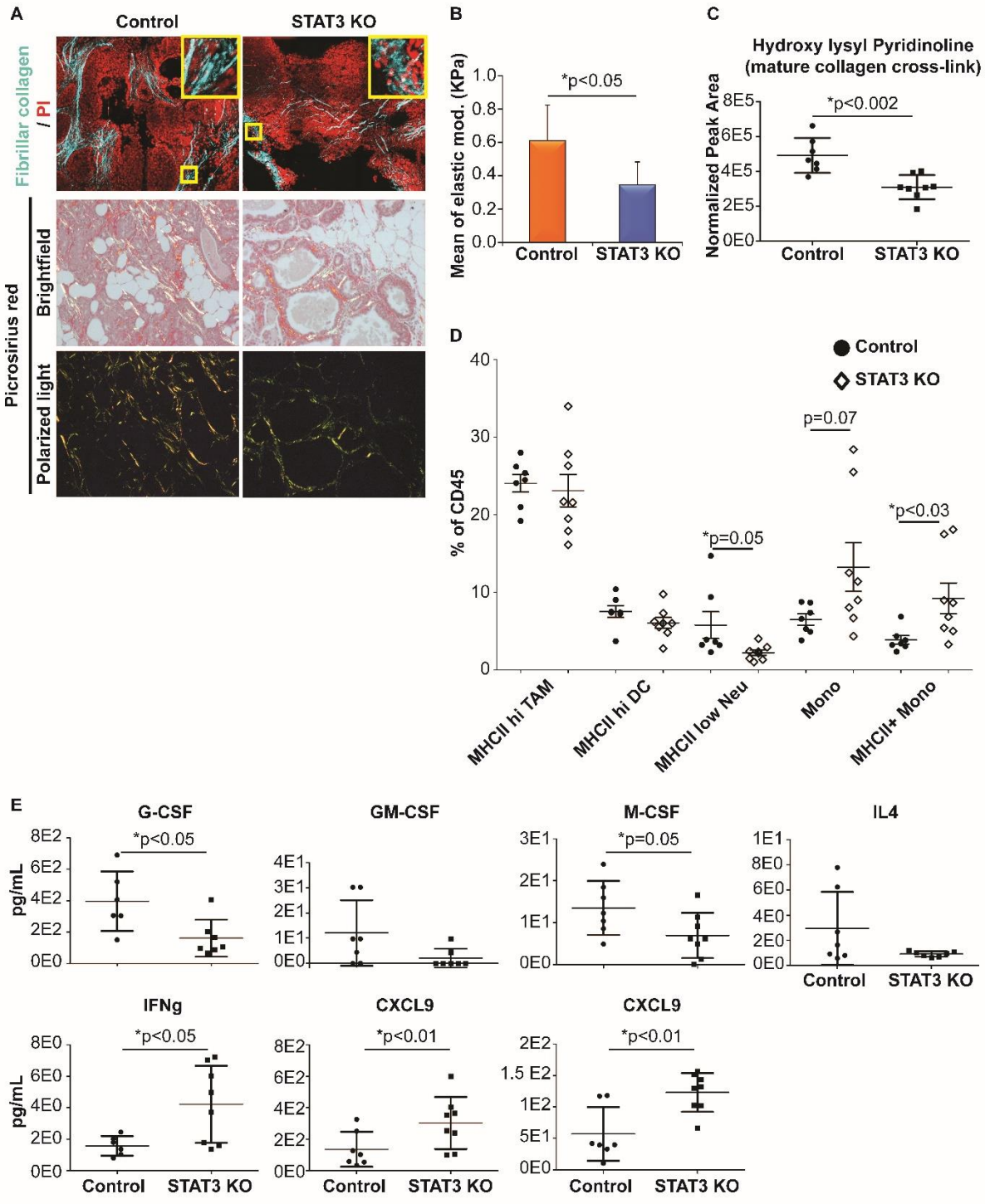
A
Control
STAT3 KO
Fibrillar collagen / PI
Picrosirius red
Brightfield
Polarized light
B
Mean of elastic mod. (KPa)
*p<0.05
Control
STAT3 KO
C
Hydroxy lysyl Pyridinoline (mature collagen cross-link)
Normalized Peak Area
*p<0.002
Control
STAT3 KO
D
Control
STAT3 KO
% of CD45
p=0.07
*p=0.05
*p<0.03
MHCII hi TAM
MHCII hi DC
MHCII low Neu
Mono
MHCII+ Mono
E
G-CSF
*p<0.05
GM-CSF
M-CSF
*p=0.05
IL4
pg/mL
Control
STAT3 KO
IFNg
*p<0.05
CXCL9
*p<0.01
CXCL9
*p<0.01

Figure 9

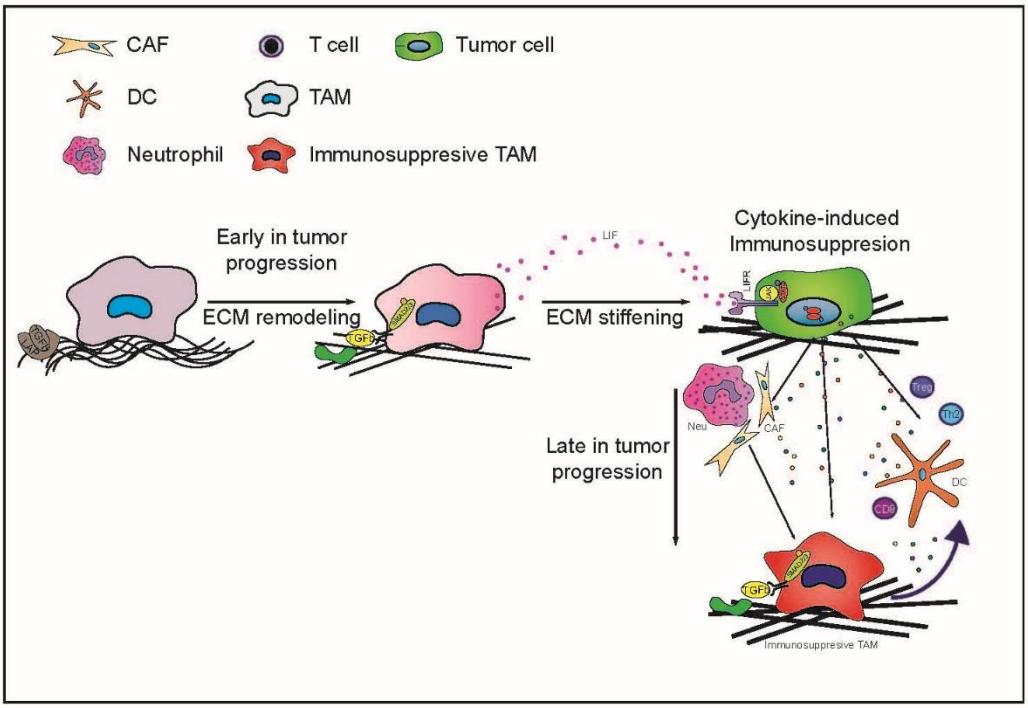
CAF
T cell
Tumor cell
DC
TAM
Neutrophil
Immunosuppresive TAM
Early in tumor progression
ECM remodeling
LIF
ECM stiffening
Cytokine-induced Immunosuppresion
LIFR
Neu
CAF
Late in tumor progression
Treg
Th2
DC
CD8
TGFβ
Immunosuppresive TAM

Supplementary Figures:

Suppl Figure 1

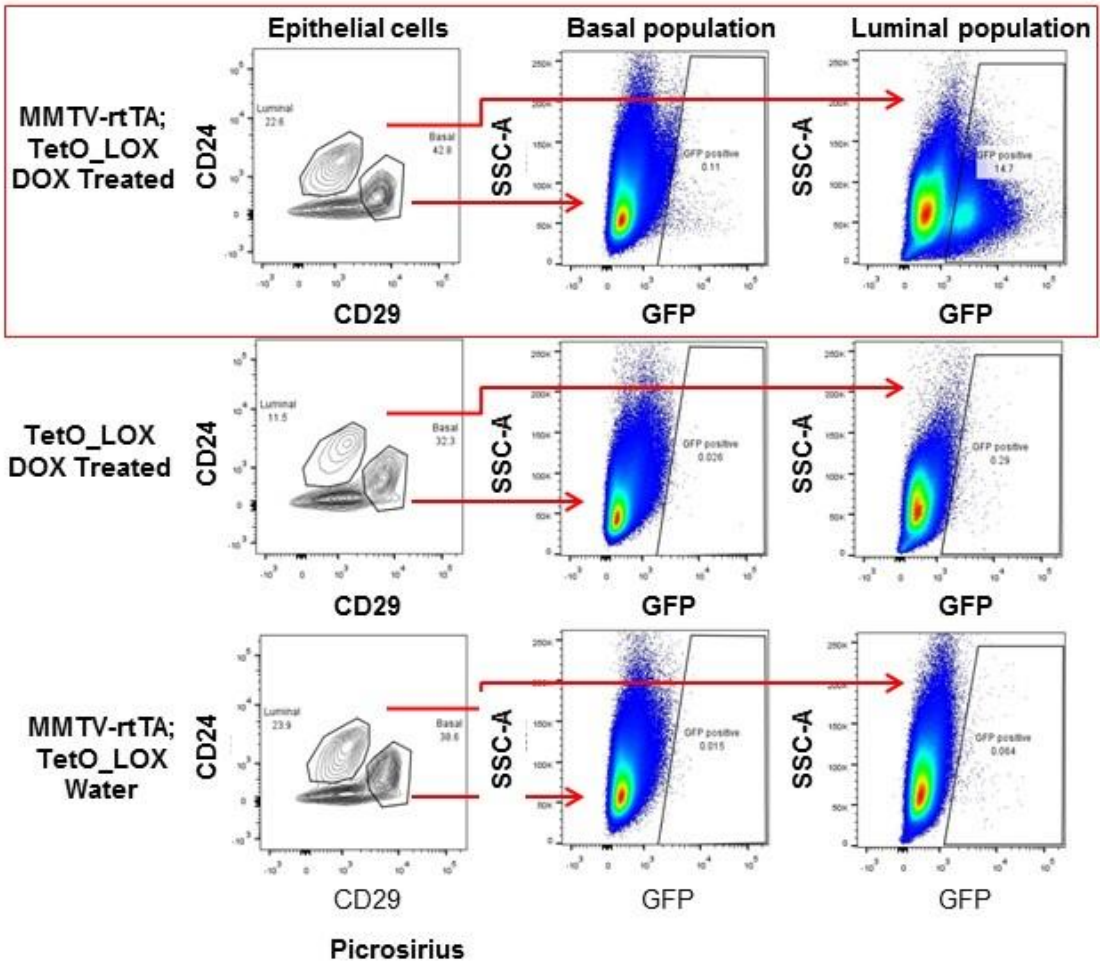

Suppl Figure 2

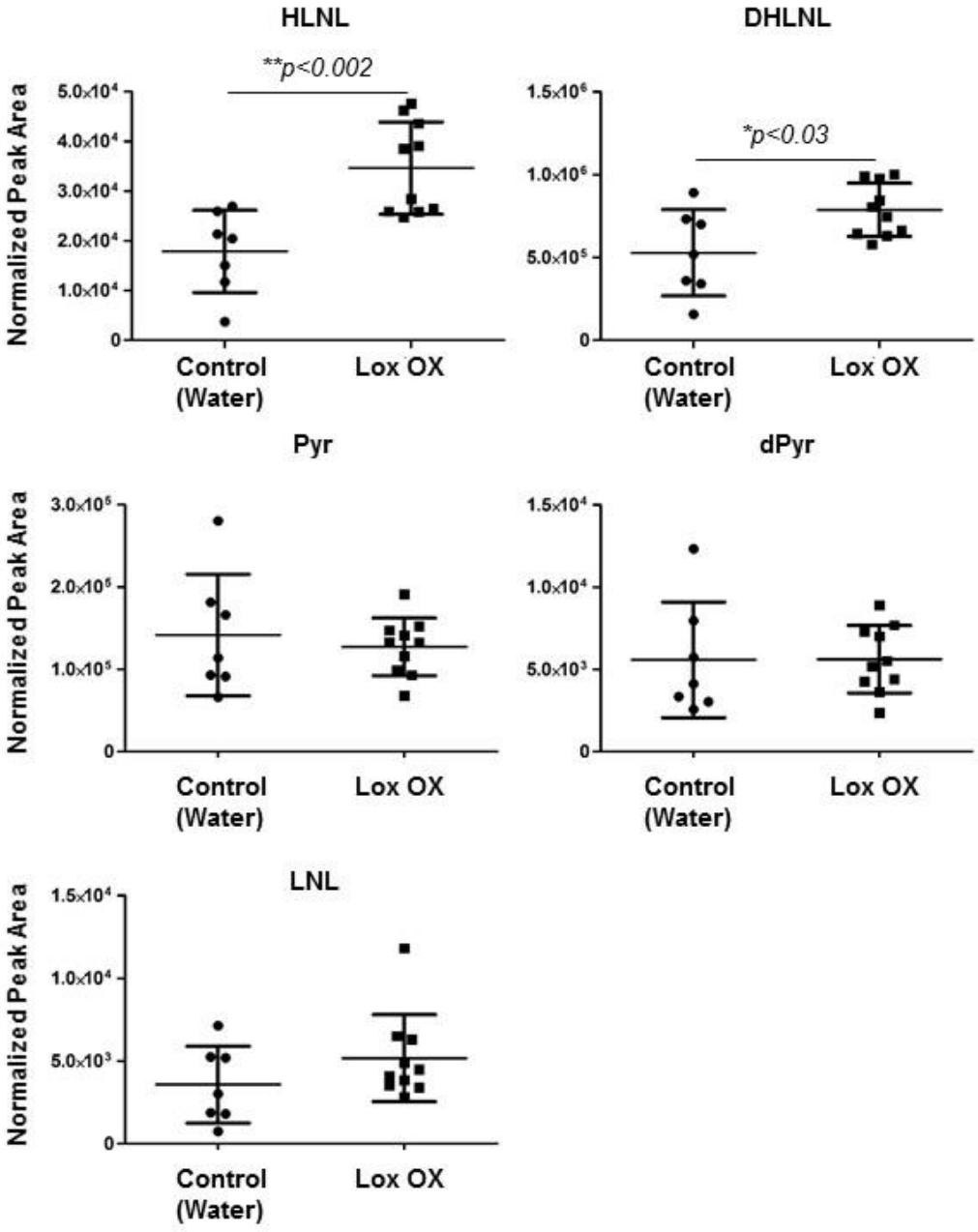

Suppl Figure 3

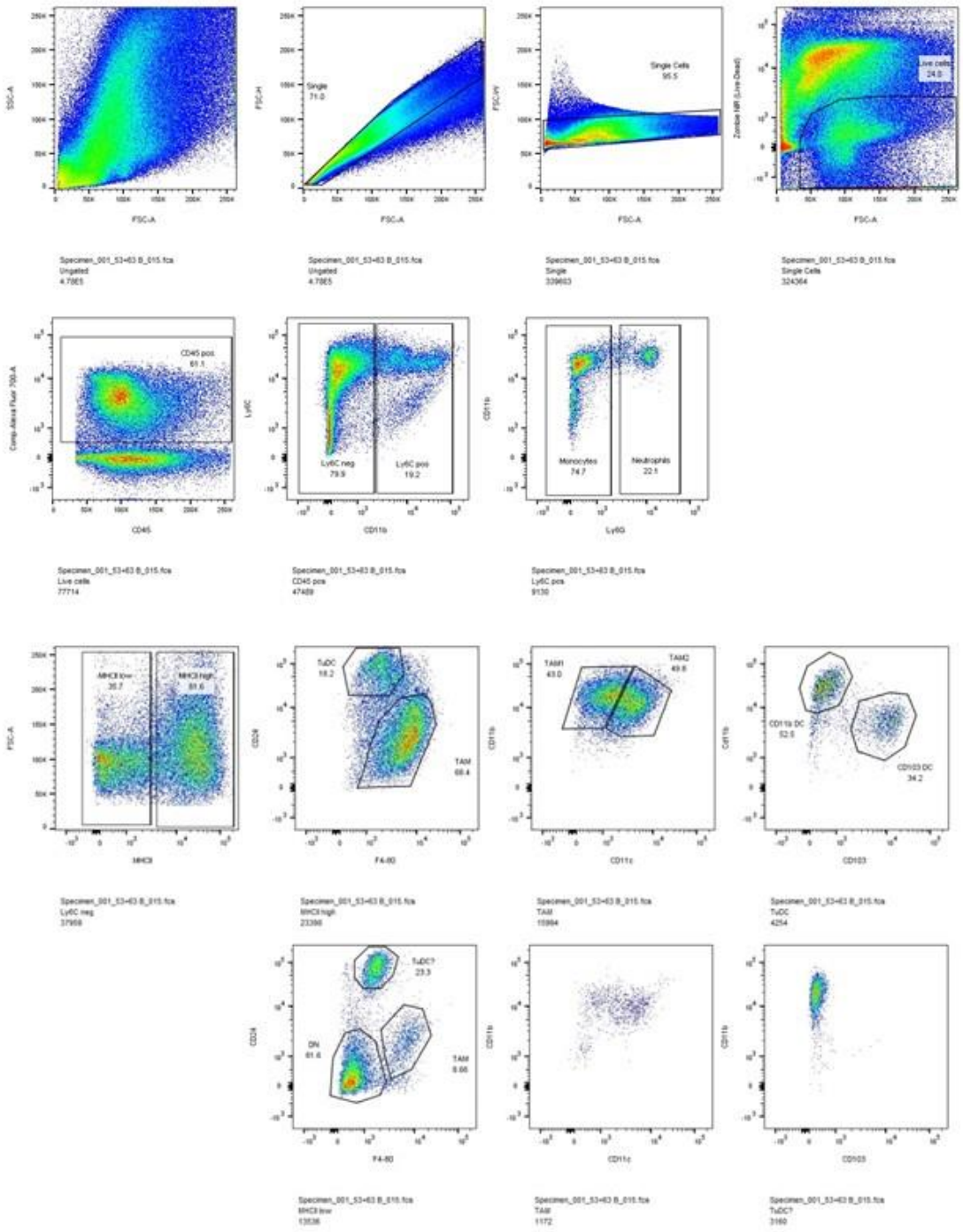

Suppl Figure 4

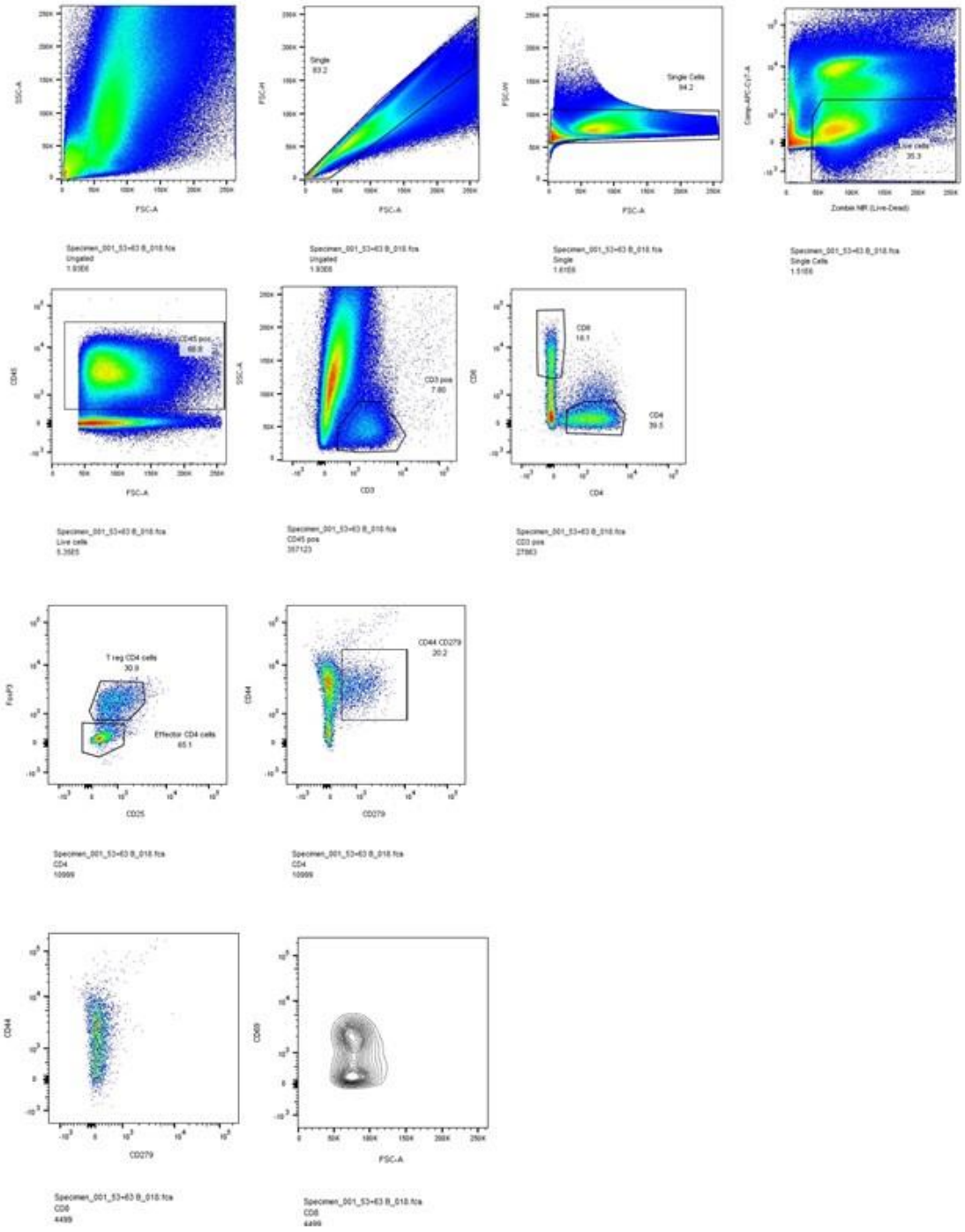

Suppl Figure 5

A.

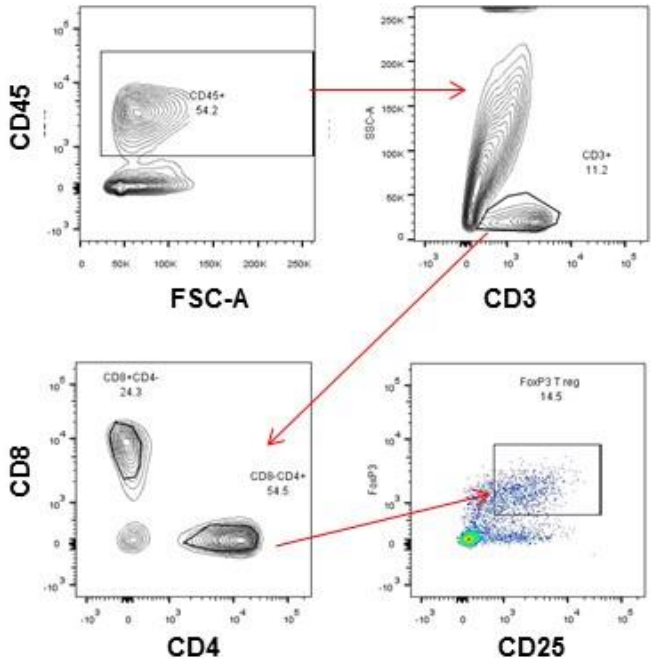

B.

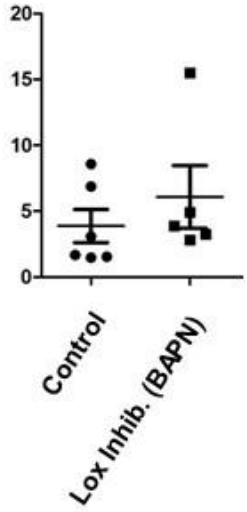

C.

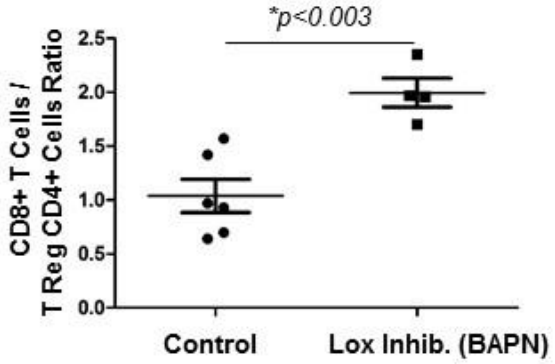

Suppl Figure 6

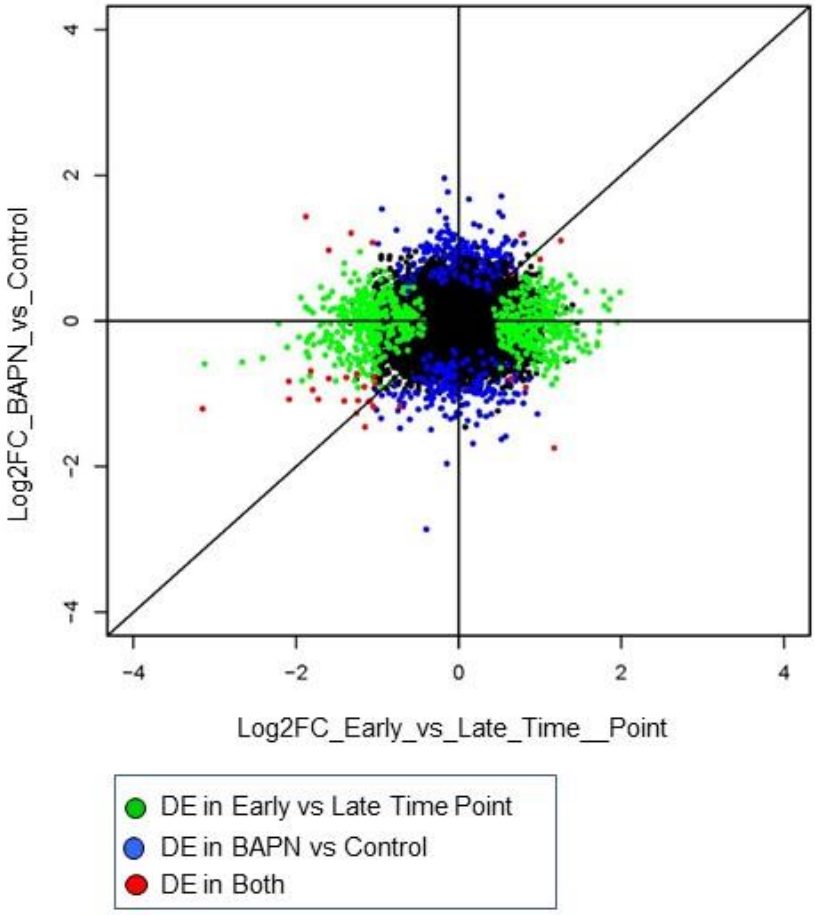

Suppl Figure 7

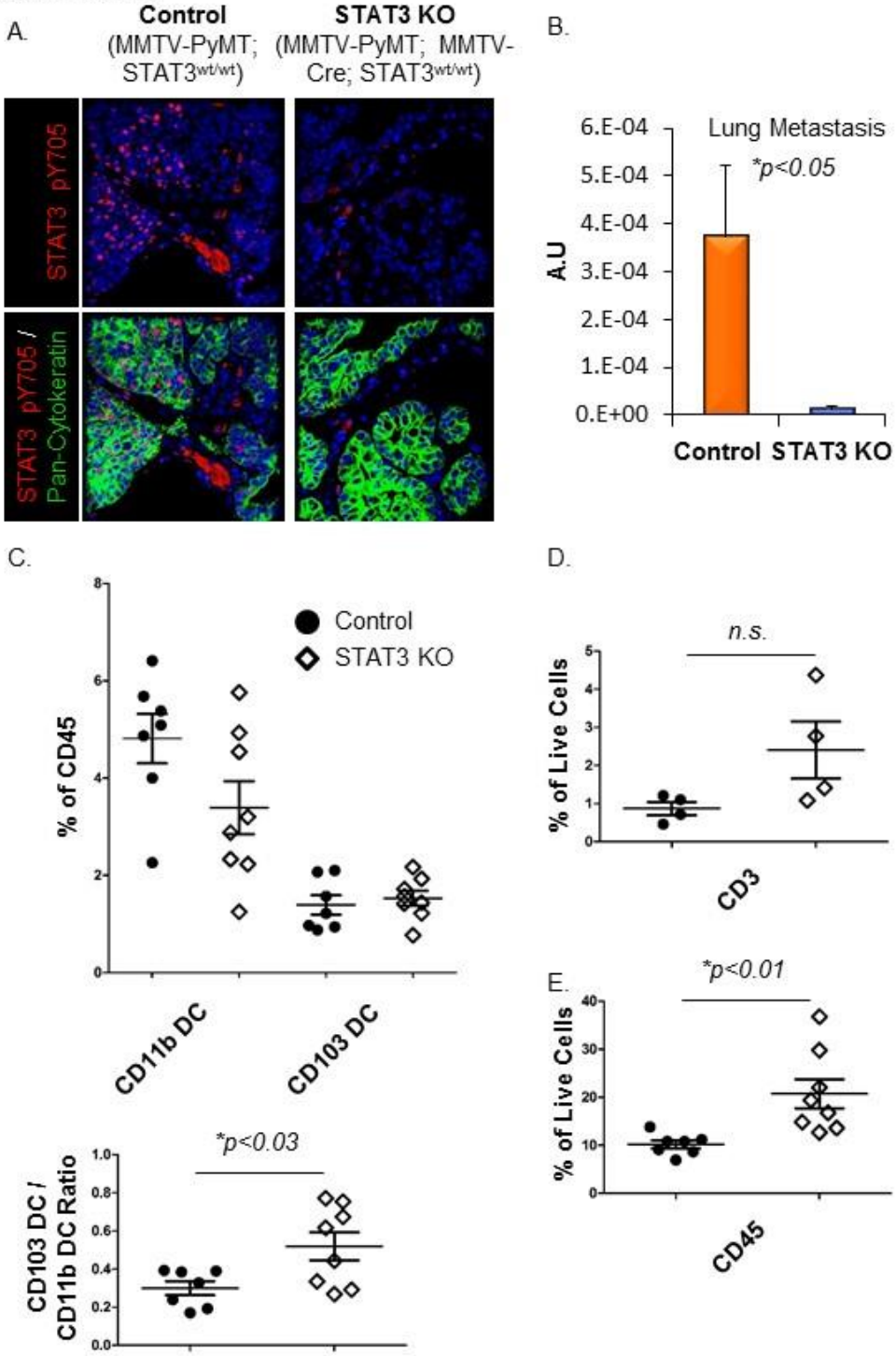

Suppl Figure 8

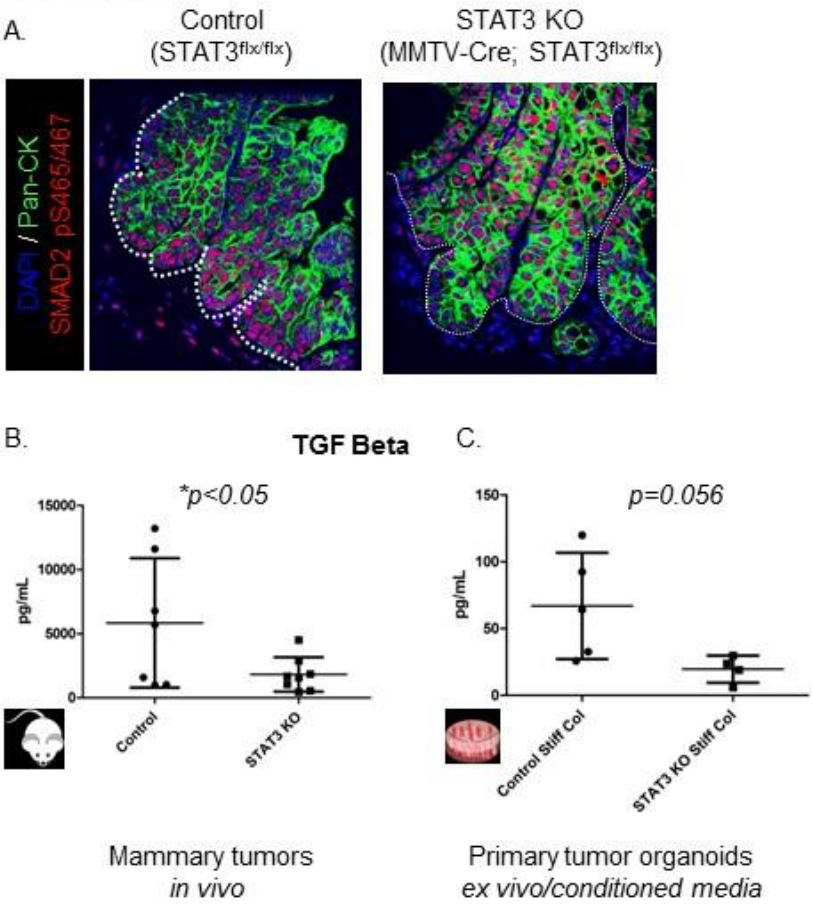

Suppl Figure 9

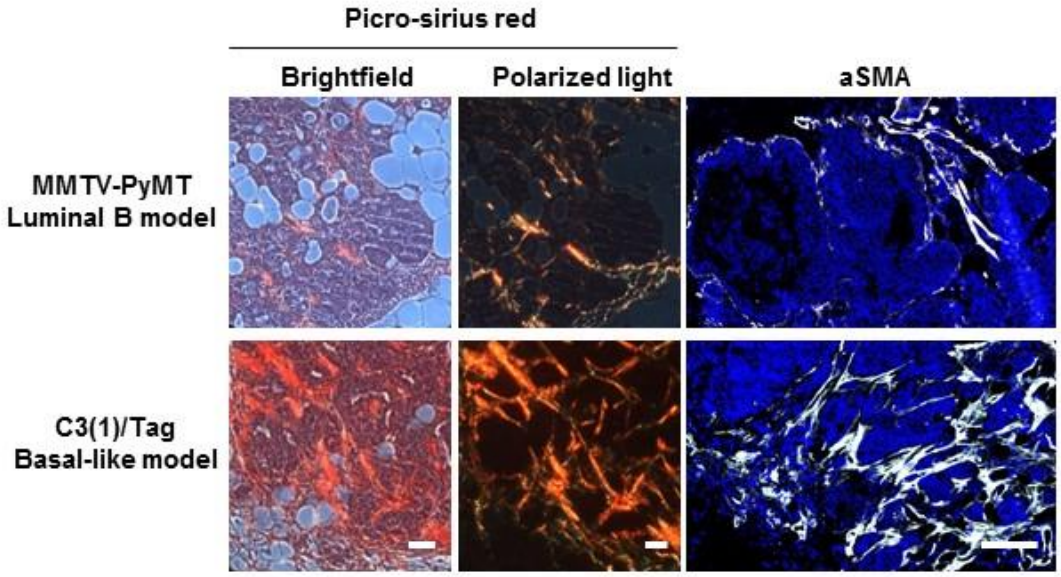

Suppl Figure 10

A.

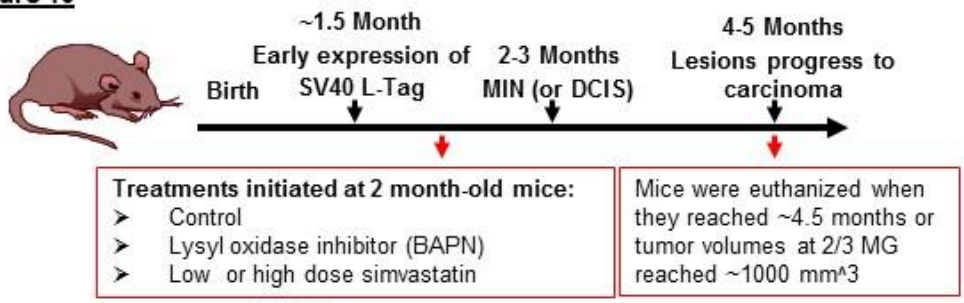

B.

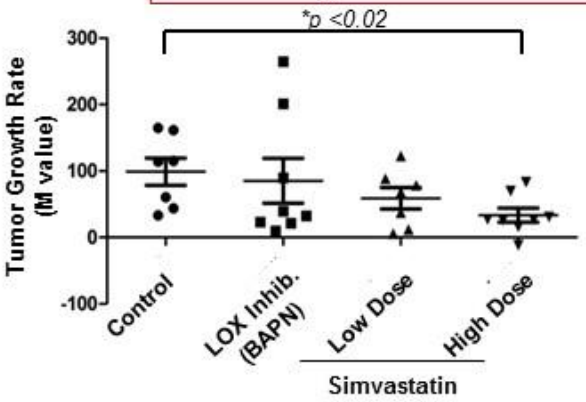

C.

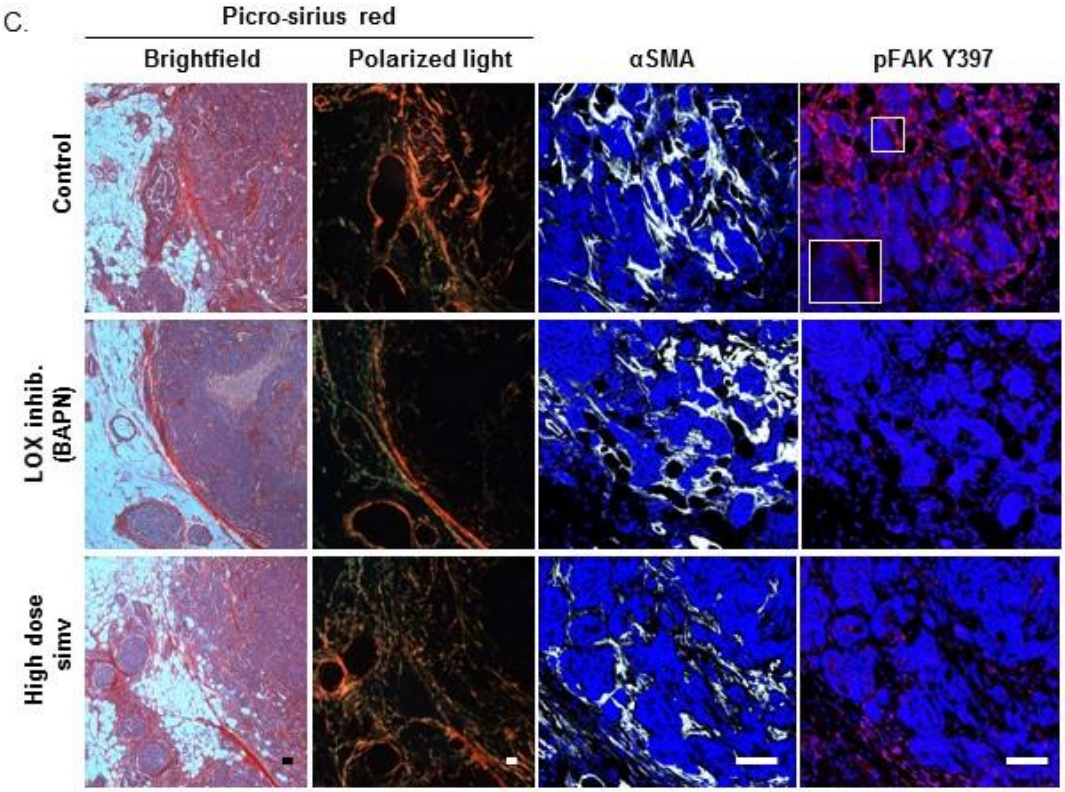

Suppl Figure 10, con't

D.

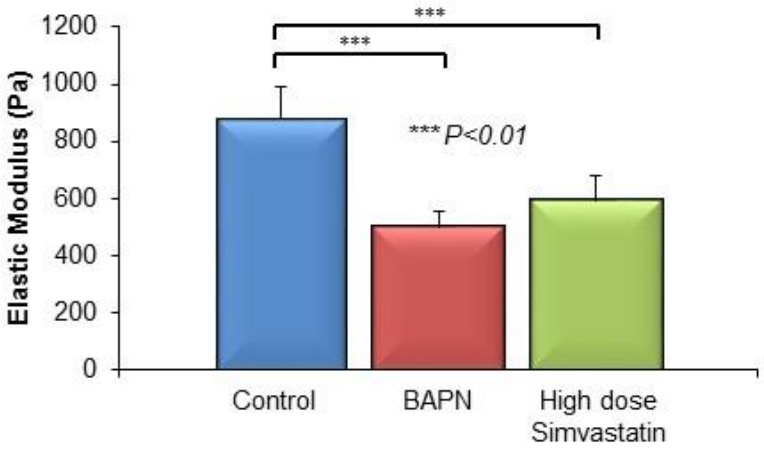

Suppl Figure 11

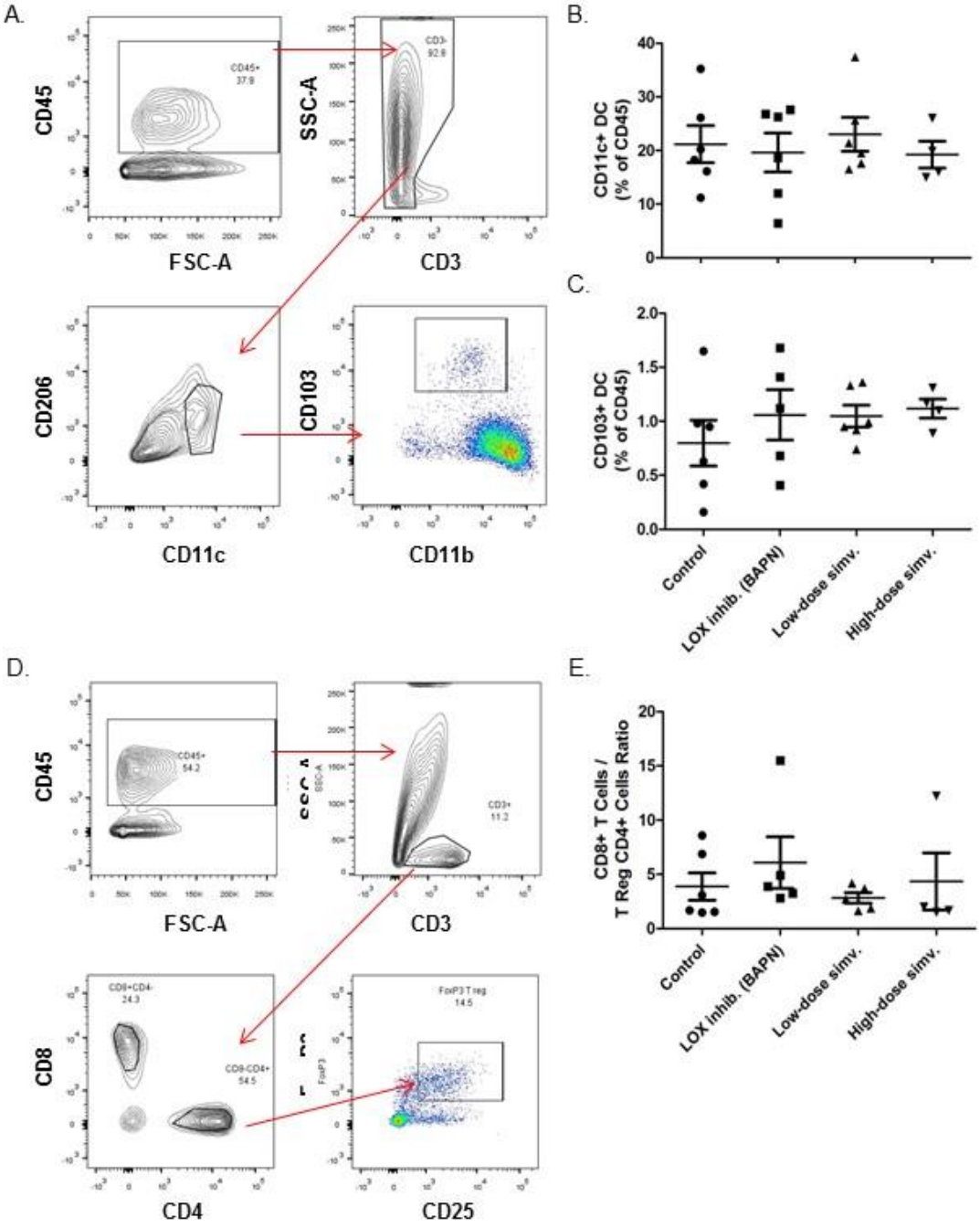

Professional development:

Key training and technical accomplishments:

1) I gained an extensive experience in immune cell profiling and sorting.
2) I completed a specialized AFM course at Aslyum (Santa Barbara, CA) arranged by Dr. Weaver.
3) I became proficient at performing 2 photon imaging on tissue samples and 3D collagen gels.
4) I successfully characterized multiple novel transgenic models to study the role of tissue mechanics in breast cancer progression.
5) I presented our work in multiple local and international conferences during my current funding year — 4 poster presentations and 3 oral presentations by the end of this calendar year.

Key leadership roles:

1) I am a point of contact for our collaborations with: 1) Dr. Hansen (University of Colorado) on ECM proteomics and collagen cross-linking assay development; 2) Dr. Lisa Coussens (OHSU) on immune cell composition and fibrosis in mouse models of luminal B breast cancer; and 3) Dr. Matthew Krummel (UCSF) on the interplay between T cell function and fibrosis in mouse model of TNBC/ basal-like breast cancer.
2) I had the opportunity to mentor multiple graduate students.

Impact:

Nothing to Report

Products:

We are planning to submit two manuscripts to top-tier journals by the end of this calendar year or beginning of 2017:

- **Ori Maller**, Luke Cassereau, Allison Drain, Brian Ruffell, Irene Acerbi, Miranda L. Broz, Jennifer M. Munson, Melody A. Swartz, Matthew F. Krummel, Lisa M. Coussens, and Valerie M. Weaver. *A role for fibrosis in promoting pro-tumor immune response in breast cancer.* **In preparation.**

- Alexander S. Barrett‡, **Ori Maller‡**, Jonathon N. Lakins, Irene Acerbi, J. Matthew Barnes, Yunn-Yi Chen, E. Shelley Hwang, Valerie M. Weaver, Kirk C. Hansen*. A novel mass spectrometry method identifies a close association between LH2-derived collagen crosslinks and poor prognosis in basal-like breast cancer.* **In preparation.**
  ‡ These authors contributed equally.

Participants & Other Collaborating Organizations:

Name:	Allison Drain
Institution:	UCSF
Project Role:	Graduate Student in Dr. Weaver's lab
Researcher Identifier (e.g.ORCID ID):	Not known
Nearest person month worked:	2
Contribution to project:	Ms. Drain is currently helping me with *in vitro* experiments
Funding Support:	Not known

Name:	Luke Cassereau
Institution:	UCSF
Project Role:	Graduate Student in Dr. Weaver's lab
Researcher Identifier (e.g.ORCID ID):	Not known
Nearest person month worked:	None this current funding year
Contribution to project:	Mr. Cassereau helped with the experiments involved polyacrylamide gels and AFM
Funding Support:	NRSA F31

Name:	Lisa M. Coussens
Institution:	OHSU
Project Role:	Collaborator
Researcher Identifier (e.g.ORCID ID):	Not known
Nearest person month worked:	N/A
Contribution to project:	Dr. Coussens's lab performed anti-CSF1 Ab treatment experiment, but we did all the analyses.
Funding Support:	Not known

Name:	Kirk C. Hansen
Institution:	University of Colorado
Project Role:	Collaborator
Researcher Identifier (e.g.ORCID ID):	Not known
Nearest person month worked:	N/A
Contribution to project:	Dr. Hansen's lab measured arginine levels and collagen crosslinking in tumor tissues.
Funding Support:	NIH R33

Name:	Matthew F. Krummel
Institution:	UCSF
Project Role:	Collaborator
Researcher Identifier (e.g.ORCID ID):	Not known
Nearest person month worked:	N/A
Contribution to project:	Dr. Krummel consulted on designing immune cell panel.
Funding Support:	Not known

Special Reporting Requirements:

Nothing to Report

Appendices

Conference: Tenth AACR-JCA Joint Conference on Breakthroughs in Cancer Research: From Biology to Therapeutics
Dates: February 16 - 20, 2016
Location: Hyatt Regency Maui, Maui, Hawaii, USA
Link: AACR program

Breaking the tension: investigating a link between tissue mechanics and tumor immunity in breast cancer

Ori Maller, Luke Cassereau, Brian Ruffell, Jason Northey Irene Acerbi, Ryan Hill, Miranda L. Broz, Jennifer M. Munson, Melody A. Swartz, Kirk Hansen, Matthew F. Krummel, Lisa M. Coussens, and Valerie M. Weaver

Human breast tumors are highly fibrotic and their extracellular matrices (ECMs) are stiffer relative to benign lesions. A major contributor to tumor mechanics is fibrillar collagen-rich ECM. During tumor progression, fibrillar collagen content increases and its organization is characterized by bundles of aligned collagen fibers that are oriented perpendicular, particularly on the invasive fronts in both mouse models of breast cancer and human disease. We previously demonstrated that a stiffened ECM and elevated mechanosignaling (e.g. β1 integrin-focal adhesion kinase signaling axis) promoted mammary tumorigenesis, whereas reducing ECM stiffening impeded tumor formation. More recently, we established a positive correlation between the number and location of infiltrating CD45 and CD68 immune cells and ECM stiffness in human breast tumors. In addition, infiltrating immune cells have been previously implicated in ECM remodeling associated with mammary gland development and tumorigenesis using mouse models. This has led us to hypothesize that tumor-associated macrophages (TAMs) drive tissue fibrosis and subsequently may stimulate inflammatory signaling.

Using the MMTV-PyMT model, early macrophage depletion not only ablated lung metastases, but demonstrated an anti-fibrotic role for TAMs depicted by a decrease in fibrillar collagen deposition and a reduction in ECM stiffness. Interestingly, CSF1 antagonist reduced phospho-STAT3 levels and FAK signaling in mammary tumors. To further substantiate the effect of tissue fibrosis on inflammatory signaling in mammary tumor cells, we inhibited lysyl oxidase (LOX), a collagen crosslinking enzyme, in MMTV-PyMT mice to attenuate ECM stiffness — we determined phospho-STAT3 levels decreased in mammary tumor cells in the treated mice in accordance with the macrophage depletion data. Lastly, we demonstrated that ECM stiffness directly caused STAT3 phosphorylation in tumor cells *in vitro* by using ECM-coated polyacrylamide gels. We also found that LOX inhibitor treatment caused a shift in the cytokine milieu consistent with an anti-tumor immune response. Furthermore, when mammary tumor cells lacked STAT3, we observed marked decreases in ECM deposition and stiffness *in vivo*. Similar to the LOX inhibition study, mammary tumors lacked STAT3 had a cytokine profile consistent with an anti-tumor immune response, suggesting a causal relationship between tissue mechanics, STAT3 signaling, and changes in cytokine milieu. Importantly, we also found that primary tumor organoids isolated from MMTV-PyMT mice embedded in stiff collagen gels induced macrophage invasion and TGFβ-mediated polarization, but not when these tumor organoids embedded in soft collagen gels.

Collectively, our data provide multiple lines of evidence to argue that macrophage infiltration promotes fibrosis that stimulates inflammatory signaling in tumor cells in early mammary tumorigenesis — and this feed-forward loop induces a pro-tumor immune response. These findings suggest that early treatment with an anti-fibrotic agent could mitigate immune suppression associated with late tumorigenesis and may enhance the efficacy of immunotherapy. In fact, we are now in the midst of demonstrating the effects of low-cost and well-tolerated anti-fibrotic agent on the immune component utilizing a mouse model of a basal-like breast cancer.

Acknowledgement: US DOD BCRP Postdoctoral Fellowship W81XWH-14-1-0056 (O.M.), US NIH T32 CA 108462-10 (O.M.), US NIH/NCI F31 CA183255 (L.C.), ARCS Foundation Fellowship (L.C.), US DOD BCRP W81XWH-05-1-0330 and W81XWH-13-1-0216 (V.M.W.), Susan G. Komen Postdoctoral Fellowship PDF12230246 (I.A.), US NIH/NCI R01 CA192914-01 (V.M.W.), NIH/NCI R01 CA174929 (V.M.W. and C.P.), Susan G. Komen KG110560PP (V.M.W. and, E.S.H. and L.M.C.) and KG111084 (E.S.H and L.M.C.), US NIH/NCI U54CA163123 and R01 CA155331 (L.M.C.), US DOD BCRP W81XWH-10-BCRP-EOHS-EXP (L.M.C.), and US BCRF A124232 (L.M.C.)

Conference: Second CRI-CIMT-EATI-AACR International Cancer Immunotherapy Conference: Translating Science into Survival
Dates: September 25 - 28, 2016

Location: Sheraton New York Times Square Hotel, New York, New York, USA

Link: AACR Conference

A role for fibrosis in promoting pro-tumor immune response in breast cancer

Ori Maller, Luke Cassereau, Allison Drain, Brian Ruffell, Irene Acerbi, Miranda L. Broz, Jennifer M. Munson, Melody A. Swartz, Matthew F. Krummel, Lisa M. Coussens, and Valerie M. Weaver

We established a positive correlation between a fibrotic phenotype in human breast tumors — especially the HER2 and Basal-like breast cancer subtypes — and CD45 and CD68 positive immune cell infiltration. We were interested in elucidating how this fibrotic phenotype may influence the immune response. To address this question, we examined if matrix stiffness alters the function of STAT3, a central regulator of tumor inflammation. We hypothesize that tissue fibrosis promotes STAT3 signaling in mammary tumor cells, and subsequently alters cytokine milieu to induce a pro-tumor immune response.

We found that ECM stiffness directly enhanced STAT3 phosphorylation in tumor cells both in vitro and in vivo. Our data suggest the fibrotic phenotype promotes STAT3 activity, enhancement of which may drive a pro-tumor immune response. Indeed, we observed several alterations in cytokines and immune cell populations upon STAT3 ablation consistent with anti-tumor immune response. Interestingly, our data also suggest STAT3 ablation in tumor cells doesn't necessary influence immune cell infiltration, but rather their differentiation in mammary tumors. Finally, we investigated if matrix stiffness has potentiated macrophage differentiation when cultured with specific immunosuppressive cytokines.

Overall, our work reveals a novel mechanistic insight into how a pro-tumor immune response stems from the interplay between fibrosis and STAT3 signaling in tumor cells. As such, our findings may stimulate an interest in exploring combinational treatment options with anti-fibrotic agents and immunotherapy.

Acknowledgements: US DOD BCRP Postdoctoral Fellowship W81XWH-14-1-0056 (O.M.), US NIH T32 CA 108462-10 (O.M.), US NIH/NCI F31 CA183255 (L.C.), ARCS Foundation Fellowship (L.C.), US DOD BCRP W81XWH-05-1-0330 and W81XWH-13-1-0216 (V.M.W.), Susan G. Komen Postdoctoral Fellowship PDF12230246 (I.A.), US NIH/NCI R01 CA192914-01 (V.M.W.), NIH/NCI R01 CA174929 (V.M.W. and C.P.), Susan G. Komen KG110560PP (V.M.W. and, E.S.H. and L.M.C.) and KG111084 (E.S.H and L.M.C.), US NIH/NCI U54CA163123 and R01 CA155331 (L.M.C.), US DOD BCRP W81XWH-10-BCRP-EOHS-EXP (L.M.C.), and US BCRF A124232 (L.M.C.)